MISS ASCELINA KATHARINA MARIA HASBERG (Orcid ID : 0000-0002-1482-6044)

DR. JANNA JUST (Orcid ID : 0000-0002-5257-604X)

Article type : Original Manuscript

Modern sedimentation processes in Lake Towuti, Indonesia, revealed by the composition of surface sediments

ASCELINA KATHARINA MARIA HASBERG[*], SATRIA BIJAKSANA[†], PETER HELD[*], JANNA JUST[*], MARTIN MELLES[*], MARINA A. MORLOCK[‡], STEPHAN OPITZ[§], JAMES M. RUSSELL[¶], HENDRIK VOGEL[‡] and VOLKER WENNRICH[*]

*Institute of Geology and Mineralogy, University of Cologne, Zülpicher Str. 49a, 50674 Cologne, Germany (E-mail: hasberg.ascelina@uni-koeln.de)
[†]Faculty of Mining and Petroleum Engineering, Institut Teknologi Bandung, Jalan Ganesa 10, Bandung, 40291, Indonesia
[‡]Institute of Geological Sciences & Oeschger Centre for Climate Change Research, University of Bern, Baltzerstr. 1+3, 3012 Bern, Switzerland
[§]Geographical Institute, University of Cologne, Zülpicher Str. 45, 50674 Cologne, Germany
[¶] Department of Earth, Environmental, and Planetary Sciences, Brown University, 324 Brook St. BOX, 1846, Providence, RI 02912, USA

Associate Editor – Ola Kwiecien

Short Title – Modern sedimentation in Lake Towuti

ABSTRACT

Lake Towuti on Sulawesi Island, Indonesia, is located within the heart of the Indo-Pacific Warm Pool. This tropical lake is surrounded by ultramafic (ophiolitic) rocks and lateritic soils that create a unique ferruginous depositional setting. In order to understand modern sediment deposition in Lake Towuti, a set of 84 lake surface sediment samples was collected

from across the entirety of the lake and samples were analyzed for their physical, chemical, mineralogical and biological constituents. End-member analyses were carried out to elucidate modern sediment origin, transport and depositional processes. This study found that allochthonous sediment, characterized by the concentrations of the elements Mg, Fe, Si and Al, as well as the clay and serpentine minerals, is dominated by fluvial supply from five distinct source areas. Granulometric data and the occurrence of organic matter of terrestrial origin suggest that in the southern and north-eastern parts of the lake the near-shore sediments may additionally be influenced by mass wasting. This at least is partly due to the particularly steep slopes in these areas. Furthermore, sediment composition suggests that sediment transport into deeper parts of the lake, particularly in the northern basin, is partly controlled by gravitational and density-driven processes such as turbidity currents. Directional sediment transport by persistent lake currents, in contrast, appears less important. Organic matter deposition in the ultra-oligotrophic lake, albeit limited, is dominated by autochthonous production, but with some contribution of fluvial and gravitational supply. Biogenic silica deposition, primarily from diatom frustules and sponge spicules, is very limited and is concentrated in only a few areas close to the shoreline that are characterized by shallow waters, but away from the areas of high suspension loads at the mouths of the major inlets. The results of this study build upon current and published work on short piston cores from Lake Towuti. Conversely, the results will support the interpretation of the depositional history and past climatic and environmental conditions derived from the composition of much longer records, which were obtained by the Towuti Drilling Project in May 2015 and are currently under investigation.

Keywords Indo-Pacific Warm Pool (IPWP), Lake Towuti, modern sedimentation, provenance analysis, redox conditions, tropical lake.

INTRODUCTION

The Indo-Pacific Warm Pool (IPWP) is the most extensive warm water mass in the world´s oceans, and houses the largest zone of deep atmospheric convection on Earth. The IPWP impacts global climate through its influence on the concentration of atmospheric water vapour, the Earth's most important greenhouse gas (Pierrehumbert, 1999) and through interactions with the El Niño–Southern Oscillation (ENSO), the Australian-Asian monsoons and the Intertropical Convergence Zone (ITCZ; Clement et al., 2001; Chen and Cane 2008; Chiang 2009). Lake Towuti on Sulawesi Island, Indonesia, is the largest tectonic lake in Southeast Asia, and sits at the heart of the IPWP. Lake Towuti has very high rates of biological endemism, with species flocks of fishes, snails and shrimp, among others (von Rintelen et al., 2011). Despite this endemism, Towuti is one of the least productive tropical lakes on Earth. Lake Towuti is located in a unique catchment, the East Sulawesi Ophiolite belt, and lateritic soils, providing ferruginous metal substrates that feed a diverse, exotic microbial community in the lake and its sediments.

Given this extraordinary setting, the Towuti Drilling Project (TDP) of the International Continental Scientific Drilling Program (ICDP) recovered over 1000 m of sediment core from three sites in the northern basin of Lake Towuti to investigate: (i) the understanding of the long-term environmental and climatic change in the tropical western Pacific; (ii) the impacts of geological and environmental changes on the biological evolution of aquatic taxa; and (iii) the geomicrobiology and biogeochemistry of metal-rich, ultramafic-hosted lake sediment (Russell et al., 2016).

The multi-disciplinary investigation of ICDP lake cores will strongly benefit from a thorough understanding of modern processes of sediment formation in this area under known environmental and climatic conditions. The most important triggering factors of sediment formation like fluvial input, terrestrial run-off and authigenic formation vary significantly in each lake. This has been shown for ICDP projects on Lake Ohrid in Macedonia/Albania and Lake El´gygytgyn in the Russian Arctic (Vogel et al., 2010; Wennrich et al., 2013). These studies have highlighted an important role for lake circulation and lateral transport in controlling and to some extent homogenizing spatial patterns of clastic and chemical sediment deposition within these lakes, as well as a role for organic matter, iron oxides and metal adsorption in chemical sedimentation. These findings helped to develop chemical tracers for tectonic and lake circulation changes (e.g. Wennrich et al., 2013). Previous work on Lake Towuti by Costa et al. (2015), Weber et al. (2015) and Goudge et al. (2017) investigated the chemical and mineralogical composition of river inputs to the lake, and developed potential tracers for sediment inputs from the largest river entering the lake, the Mahalona River. However, those studies were limited by very low areal coverage (only one sediment transect in the northern lake basin; Fig. 1), and did not investigate spatial gradients in organic matter or other patterns of chemical sedimentation. It is possible that the low-latitude setting and ultra-oligotrophic status of Lake Towuti limit the effects of in-lake circulation and organic matter production on the spatial patterns of sediment infill in Lake Towuti; however, this has yet to be tested through comprehensive sampling and analysis.

In this study, 84 lake surface sediment samples were collected from Lake Towuti to document patterns of sedimentation over the entire lake basin. These samples were investigated for a variety of physical, mineralogical and chemical attributes. The results presented here shed new light on the modern sedimentary processes operating in Lake Towuti

and complement studies which focus on modern weathering processes in the lake catchment and potential analogues to iron-rich lake sediments observed on Mars. Furthermore, this study provides information concerning potential impact of anthropogenic activity during recent decades on the composition of the surface sediments in Lake Towuti, in particular the impacts of extensive nickel mining to the north-west of the lake (PT Vale, 2017), population increase in expanding villages (Robinson, 1986), as well as increased deforestation and farming in the lake catchment (Dechert et al., 2004).

STUDY SITE

Lake Towuti is part of the Malili Lake System, a chain of five lakes in the centre of Sulawesi Island, north-eastern Indonesia (2.5°S, 121.5°E; Fig. 1). The three largest of these lakes are connected by surface outflow from Lake Matano via Lake Mahalona to Lake Towuti, with the latter located at 319 m above sea level and draining into the Bay of Bone via the Larona River. The 561.1 km^2 large, and *ca* 200 m deep Lake Towuti occupies a transtensional basin (Lehmusluoto et al., 1995; Haffner et al., 2001) situated at the junction of the Eurasian, Caroline–Philippine and Indo–Australian tectonic plates (Hamilton, 1979; Spakman and Hall, 2010). Frequent earthquakes (168 between 2010 and 2016), including several above magnitude five, highlight modern tectonic activity (Watkinson and Hall, 2016). Moreover, subduction under North Sulawesi leads to an extensive volcanic field on the island's northern arm, which has been active since the Miocene (Hamilton et al., 1979).

The majority of the catchment area of Lake Towuti (1280 km^2) consists of mafic to ultramafic bedrock of the East Sulawesi Ophiolite belt, the third largest ophiolite complex in the world (Fig. 2; Monnier et al., 1995; Kadarusman et al., 2004). The ophiolites around Lake Towuti are composed primarily of serpentinized (lherzolite) and unserpentinized peridotites

(harzburgite and dunite; Kadarusman et al., 2004, fig. 2), as well as minor gabbros, dolerites and basalts. The peridotites are intensely weathered and form laterites several metres thick, including nickeliferrous oxisol soils with an FeO content of about 60% (Golightly and Aranabia, 1979; Kadarusman et al., 2004). Additionally, the ophiolite is interthrusted by Mesozoic and Cenozoic sediments and metasediments (Silver et al., 1983; Kadarusman et al., 2004).

Lake Towuti is roughly separated into a northern and a southern basin by a large island and a series of subaquatic ridges ascending to *ca* 125 m water depth (Fig. 1; Russell et al., 2016;). The largest tributary is the Mahalona River, which forms a large delta in the northern part of the lake (the Mahalona Delta) and exerts a strong influence on sedimentation in the northern basin (Costa et al., 2015; Vogel et al., 2015; Weber et al., 2015; Goudge et al., 2017). Today, Lake Towuti is ultra-oligotrophic and dilute (conductivity 210 µS/cm), with a circumneutral pH (*ca* 7.8), and the water chemistry is dominated by Mg and HCO_3^- ions (Lehmusluoto et al., 1995; Haffner et al., 2001; Vuillemin et al., 2016). The lake is thermally stratified, with seasonal mixing occurring down to *ca* 100 m and surface water temperatures between 29°C and 31°C (Costa et al., 2015).

The climate at Lake Towuti is tropical humid, exhibiting a mean annual air temperature of 26°C with monthly averages varying by less than 1°C (Costa et al., 2015). Precipitation averages *ca* 2700 mm/year, with its maximum and minimum in March/April and in October, respectively, governed by the seasonal influences of the ITCZ and the Australian-Indonesian Summer Monsoon (AISM; Konecky et al., 2016). During the wet season from December to May, when precipitation can exceed 250 mm/month, the ITCZ passes over the region, northerly winds associated with the AISM prevail, and local

convective activity, triggered by warm sea-surface temperatures (SST), is high (Aldrian and Susanto, 2003). In contrast, from August to October, the atmospheric circulation is dominated by south-easterly flows, which transfer latent heat to the Asian mainland, decreasing regional SSTs and local convection, and thus decreasing precipitation around Lake Towuti below 150 mm/month (Aldrian and Susanto, 2003; Hendon 2003). The lake and its surroundings are heavily influenced by ENSO events. The El Niño event 1997/1998, for instance, led to strongly reduced precipitation during the rainy season, causing a lake-level lowering of *ca* 3 m, and a nearly closed-basin situation (Tauhid and Arifian, 2000).

Despite its importance in the global climate system, the interaction of the IPWP with climate change is still poorly constrained. To further understanding of oceanic and continental environmental conditions in the IPWP region, lake sediment cores are valuable archives as they contain highly resolved and potentially long records of climatic changes. The information presently available concerning the history of Lake Towuti is primarily based on the investigation of piston cores of up to 20 m length, which were recovered in 2010 and span the past *ca* 60,000 years (Russell et al., 2014; Vogel et al. 2015). Additional information is available from seismic data obtained in 2007, 2010 and 2013 (Russell et al., 2014; Vogel et al., 2015) as well as three TDP sites drilled in 2015, with sediment penetrations between 138 m and 174 m below lake floor (blf; Russell et al., 2016). These cores probably expand the existing records to at least 700 kyr (Russell and Bijaksana, 2012), providing a unique, high-resolution continental archive to investigate the influence of orbital forcing and northern hemisphere glaciations on climate variations within the IPWP region.

Organic geochemical and compositional analyses of the upper *ca* 10 m of the sediments indicates particularly wet conditions with closed-canopy rainforest in the catchment during Marine Isotope Stage (MIS) 3 and the Holocene (Russell et al., 2014). These conditions abruptly changed to drier conditions with more open ecosystems (seasonal forests and grasslands) during MIS 2, especially during the Last Glacial Maximum (LGM; Russell et al., 2014). The palaeoclimatic changes impacted not only the regional vegetation, but also sediment supply to the lake, water-column mixing, sediment redeposition, and lake-levels (Russell et al., 2014, 2016; Vogel et al., 2015; Costa et al., 2015; Konecky et al., 2016; Goudge et al., 2017). However, there are still many uncertainties from these studies. For instance, Russell et al. (2014) used sedimentary Ti content to infer surface runoff and erosion, whereas other studies (Costa et al., 2015; Vogel et al., 2015; Goudge et al., 2017) used sedimentary Mg content to infer sediment remobilization driven by lake-level changes. Costa et al. (2015) used Fe concentration data to infer changes in lake mixing, but lacked information about whether Fe concentrations changed across the oxycline of Lake Towuti in the present day. Improved understanding of the spatial patterns of sedimentation in the modern-day lake, and the impacts of lake circulation and heterogeneous sediment source areas will significantly facilitate the interpretation of the palaeorecord lake circulation and heterogeneous sediment source areas.

MATERIAL AND METHODS

Field work

Lake Towuti surface sediments were sampled during TDP drilling operations in May 2015. Eighty-four samples were collected from water depths between *ca* 2.8 m and *ca* 200 m (Table 1), forming a dense, high-resolution (1 to 4 km) sampling grid that covered the entire lake

(Fig. 1). Sampling was conducted using a grab sampler (UWITEC Corp., Mondsee, Austria) operated by a hand winch mounted to a local boat. Water depths at the sampling sites were measured by echo-sounder (LCX-17M; Lowrance, Tulsa, OK, USA), and the positions were determined using a hand-held global positioning system (Furuno^{TM} GPS; Furuno Electric Co. Ltd, Mishinomiya, Japan). Material was sampled from the top 5 cm of the recovered grab sample. Based on mean Holocene sedimentation rates of 0.205 mm/year at TDP Site 1 (Russell et al., 2014) and 0.235 mm/year (excluding event layers) close to TDP Site 2 (Vogel et al., 2015), the deepwater samples integrate *ca* 200 to 250 years.

On site, large organic remains; such as shells, woody twigs and leaves, were removed using tweezers and the remaining sediment was divided into four homogenized aliquots. The aliquots were stored in high-density polyethylene Whirl-pak™ sample bags or 50 ml polystyrene NUNC vials and shipped to different laboratories for individual analyses.

Analytical work

At the University of Cologne, Germany, a subsample was taken from one aliquot and used to produce smear slides for identification of sedimentary components using transmitted light microscopy. On selected samples, sponge spicules and diatom frustules were additionally investigated using a Zeiss Gemini Sigma 300VP scanning electron microscope (SEM; Carl Zeiss AG, Oberkochen, Germany). Furthermore, some magnetic mineral grains were identified with energy dispersive X-ray spectroscopy (EDX) of the Sigma SEM system.

Based on smear slide analyses, a set of 40 samples that contain sponge spicules, diatoms and/or tephra particles were selected for automated, non-destructive particle image analyses using a dynamic imaging system (Benchtop B3 Series VS FlowCAM®; Fluid Imaging Technologies Inc., Scarborough, ME, USA) to quantify the abundance of these particles. Aliquots of wet bulk samples were treated with hydrogen peroxide (H_2O_2; 30%) for seven days at room temperature to remove organic matter (OM) and disaggregate the siliceous biogenic particles, and were subsequently sieved with 25 µm and 80 µm meshes. The pre-treated sample fractions were diluted with deionized water (samples <25 µm) or polyvinyl pyrrolidone (PVP, 2%; samples 25 to 80 µm and >80 µm). Particle recording in the <25 µm and 25 to 80 µm fractions was carried out using a 100 µm flowcell, a 10x objective lens with a collimator, and a 1 ml syringe-pump (flow rate 0.3 ml/min), whereas the >80 µm fraction was recorded using a 300 µm flowcell, a 4x objective lens without collimator, and a 5 ml syringe-pump (flow rate 0.6 ml/min). Data were acquired using the software VisualSpreadsheet (Fluid Imaging Technologies Inc.) until 10 000 images were recorded or 30 ml of the sample was investigated. An automated catalogue based on training sets developed for sponge spicules, diatoms and tephra particles was compiled to differentiate and group components with comparable characteristics in the measured sample fractions.

The mass magnetic susceptibility (MS) was analyzed on wet bulk sediment aliquots using a KLY-2 Kappabridge (AGICO, Brno, Czech Republic). Magnetic susceptibility measurements were carried out on sample containers of 2.0 x 2.0 x 1.6 cm (i.e. a sample volume of 6.4 cm^3) which frequently are used for palaeo and rock magnetic measurements. The only exceptions are samples 12 and 33, which did not contain sufficient material.

For granulometric, geochemical and mineralogical analyses, approximately 25 ml of each surface sample was frozen for 24 hours and subsequently lyophilized using a Christ BETA 1-8 LDplus (Martin Christ Gefriertrocknungsanlagen GmbH, Osterode am Harz, Germany). The freeze-dried samples were homogenized and split into two aliquots. One aliquot of 1 g was used for grain-size analyses, following a three-step pre-treatment procedure adapted after Francke et al. (2013). First, OM was dissolved with 15 ml H_2O_2 (30%) in a water bath at 50°C for 18 hours. This step was repeated once to ensure that the OM was fully dissolved. Subsequently, carbonates were dissolved by treatment with 10 ml hydrochloric acid (HCl; 10%) at 50°C in a water bath for three hours, with regular shaking of the samples to ensure complete reaction. Finally, biogenic silica (bSi, opal) was dissolved by two treatments with 10 ml of sodium hydroxide (NaOH, 1 M) solution for one hour. Each step was followed by repeated centrifuging, decanting, and rinsing of the samples with deionized water until reaching a neutral pH. These pre-treated aliquots were subsequently diluted with 60 ml of deionized water, dispersed with sodium pyrophosphate ($Na_4P_2O_7$; 2.5 g/l), and placed on a shaker for at least 12 hours. The grain-size measurements were performed with a Beckman Coulter LS13320 laser particle analyzer (Beckman Coulter Life Sciences, Indianapolis, IN, USA) applying the Fraunhofer diffraction theory. For that purpose, each sample was pumped into the measurement tank of the analyzer and filled with deionized and degassed water until the sediment-water mixture reached the required transparency. Three measurements of each sample were used to calculate the average grain-size distribution. Results were calculated by averaging triplicate measurements of each sample and are given in volume percentages (vol. %) for 116 grain-size classes between 0.04 µm and 2000 µm diameter.

The other aliquot of the freeze-dried surface samples was ground to <63 µm with a Planetary Mill Pulverisette 5 (FRITSCH GmbH, Idar-Oberstein, Germany) and used for mineralogical and geochemical analyses. The bulk mineralogy was determined on powder samples using an X-ray diffractometer (D8 Discover; Bruker, Billerica, MA, USA) with a Cu X-ray tube (λ = 1.5418 Å, 40 kV, 30 mA) and a LYNXE XE detector (opening angle = 2.9464°). The spectrum from 3° to 100° 2-theta was measured in 0.02° steps at 1 second exposure time. Mineral identification was carried out using the software packages SEARCH (Stoe and Cie GmbH, Darmstadt, Germany) and Match! (Crystal Impact 2014, Bonn, Germany), supported by the data base pdf2 (ICDD 2003, Newton Square, PA, USA). The concentration of the minerals was evaluated using the program TOPAS Rietveld (Coelho Software, Brisbane, Australia), which yields a standard deviation of analyzed minerals varying from ±2% (for quartz) to ±5 to 10% (for feldspars and clay minerals; Środoń et al., 2001; Vogt et al., 2002). For the clay mineral group illite the error range can be even higher (Scott 1983). Given these uncertainties, a detection limit of 5% is considered in the discussion of the mineralogical composition of the surface sediments.

Total organic carbon (TOC**)** as well as total carbon (TC), total nitrogen (TN) and total sulphur (TS) were measured with a vario MICRO cube and vario EL cube combustion elemental analyzers (Elementar Analysesysteme Corp., Langensebold, Germany), respectively. For the TOC measurements, 15 mg of sediment powder was placed into metallic silver containers, heated to 100 to 120°C, and treated three times with a few drops of HCl (32%) to dissolve carbonates. The metallic silver containers were then wrapped and pressed into silver paper, and the resulting pellets were analyzed for their TOC concentration using the vario EL cube. All concentrations are given as mean values of duplicate measurements. For TC, TN and TS measurements with the vario MICRO cube, 10 mg of sediment powder

was placed in zinc containers, with 20 mg of tungsten (VI) oxide (WO_2) added to catalyze oxidation. The total inorganic carbon (TIC) was calculated as the difference between TC and TOC. Analytical errors were determined on internal and external reference material. The C/N ratio is calculated as the weight ratio of TOC and TN.

For quantitative analyses of the inorganic element composition of the surface samples, including concentrations of selected major, minor and trace elements (Ti, K, Al, Mg, Ca, Fe, Cr and Mn), 0.5 g of dry and ground bulk sample material was digested using a near-total digestion protocol with HCl, nitric (HNO_3), perchloric ($HClO_4$) and hydrofluoric (HF) acids in heated and closed teflon vessels. Measurements were performed by means of inductively coupled plasma-mass spectroscopy (ICP-MS) at Activation Laboratories Limited, Ancaster, ON, Canada.

Separate Si measurements were conducted by energy-dispersive X-ray fluorescence (ED-XRF) using a portable analyzer (NITON XL3t; Thermo Fisher Scientific, Waltham, MA, USA) at the University of Cologne, Germany. Triplicate measurements were performed on pellets of freeze-dried and ground sample aliquots, which were pressed into teflon rings under 12 bars, and subsequently covered with a 4 µm polypropylene film (X-ray film, TF-240-255, Premier Lab Supply, Port St. Lucie, FL, USA). Measurements were performed using a gold anode X-ray source (70 kV) and the 'mining-minerals-mode'. The secondary X-rays of element-specific photon energies were detected with a silicon drift detector and processed by a digital signal processor. Si concentrations (in ppm) were calculated from the element-specific fluorescence energies and compared with external and internal reference materials (STDS-4, BCR142R and BCR-CRM 277).

The carbon isotopic composition of bulk OM ($\delta^{13}C_{OM}$) in the sediment was measured on a set of 42 subsamples at Brown University, Providence, RI, USA. For that purpose, *ca* 50 mg of sediment was acidified in HCl (2 N) for one hour at 80ºC to remove carbonate minerals. The acid-treated samples were subsequently rinsed in deionized water and centrifuged four times to remove any excess HCl. The samples were then freeze-dried and homogenized prior to isotopic analysis. The $\delta^{13}C_{OM}$ values were measured using a Carlo Erba Elemental Analyzer coupled to a Thermo DeltaV Plus isotope ratio mass spectrometer (Thermo Fisher Scientific). The analytical precision determined through replicate measurements of internal sediment standards was 0.16‰. All results are reported relative to the Vienna Pee-Dee Belemnite (VPDB) standard.

Elevation model, interpolation and statistical analysis

A digital elevation model (DEM) of Lake Towuti and its surrounding was calculated using ArcGIS (Esri, Inc., Redlands, CA, USA). The model is based on open source satellite data for Sulawesi provided by the United States Geological Survey (Aster Global DEM based on the Shuttle Radar Topography Mission carried out by the National Aeronautics and Space Administration at 1 arc-second 30 m spatial resolution). Spatial interpolation of the analytical surface sediment data was carried out with the software Surfer 9 (Golden Software Inc., Golden, CO, USA) using the kriging method.

Statistical analyses employed on the surface sediment data sets comprise end-member (EM) unmixing, principal component analysis (PCA) and a redundancy analysis (RDA). End-member analyses were carried out on normalized and standardized grain-size (EM_{GS}), chemical (EM_{Chem}) and mineralogical (EM_{Min}) data sets. Assuming a sedimentary mixture from different sources the mixing model in all cases can be written as:

$$X = AS + E \qquad (1)$$

where X represents the *n* by *m* matrix of *n* samples (one per row) and *m* variables (relative abundance of individual data). Matrix A (*n* by *l*) denotes the mixing proportion of *l* end-members for the *n* samples, S represents the *m* properties of the *l* EMs and E is the error matrix of residuals. The uncertainties of the EM analyses are controlled by the errors of the data sets used.

The EM algorithm developed by Heslop and Dillon (2007) adopting the approach of Weltje (1997) was applied. The decision criterion of how many EMs are included in the three models is based partly on the coefficients of determination derived from the PCA. Nevertheless, the number of the respective EMs should also be reasonable in the geological context of the data set (Weltje, 1997; Weltje and Prins, 2007). Residuals of the EM models include analytical errors and non-identified additional sources of variability.

All other multivariate statistical analyses were carried out with the Excel-based software Addinsoft XLSTAT (STAT*CON* GmbH, Witzenhausen, Germany) The PCA was conducted with the sand content and the concentrations of selected elements determined by ICP-MS and XRF analyses (Fe, Mg, Al, Si, K, Ca, Cr and Ni). In the RDA, the results derived from the PCA are expanded by the concentrations of major minerals, the MS and TOC values and the C/N ratio. The correlation matrix includes all data except $\delta^{13}C_{OM}$ and the concentrations of diatom frustules, sponge spicules and tephra particles, which all were determined on a subset of the surface samples only.

RESULTS

Biological particles

The surface samples of Lake Towuti consist mostly of dark greenish-grey, structureless clastic sediments with low but varying amounts of amorphous OM, macrofossils and microfossils. Macrofossils include plant remains and wood fragments, which frequently occur in near-shore, shallow-water samples as well as a few deepwater samples in Towuti's northern basin (samples 16, 17 and 22; Table 1; Fig. 1). In addition, mollusc macrofossils were observed in four samples (samples 18, 50, 51 and 83) that are located proximal to the shore in water depths of less than 4.5 m.

Diatom frustules and sponge spicules are the most abundant microfossils observed in the sediments (Fig. 3); they are, however, quite rare, and together average only 0.46% of the total number of the detected sediment particles, with the highest concentrations reaching 2.34% (sample 5). The concentrations of these particles relative to the total sediment mass are considerably lower, as sample pretreatment prior to particle detection enhanced their abundance. The diatom frustule content is somewhat elevated in front of the Timampu inlets at the north-western shore and in front of the Mahalona River at the northern shore, and shows pronounced maxima in front of the Tomerakah and Taora rivers at the eastern shore and along the southeastern shore near the Lengke and Lantibu rivers (Figs 2, 3A and 4A). Some of the discovered diatoms were identified as *Pinnularia sp.* and *Surirella robust var. splendida*, the latter of which is known to occur in all Malili Lakes, Lake Poso to the north-west and possibly on Java Island (Roy et al., 2007; Sabo et al., 2008; Vaillant et al., 2011; Bramburger et al., 2014).

Sponge spicules occur in two different forms, both up to 200 µm in length. One form has an ornamented surface structure with rounded ends, whereas the other is smooth with sharp tip ends (Figs 3B and C). Since both types are very similarly distributed within the lake, their abundances are shown as combined in Fig. 4B. The highest abundances of spicules were detected in the northern part of Lake Towuti, between the Mahalona and Timampu rivers, and in the eastern part of the lake, in particular in front of the Lemo-Lemo and Tomerakah rivers. Somewhat elevated values also occur at the southern shore, in front of the Tokolalo River.

Physical properties

The grain-size distribution (classification after Udden, 1914 and Wentworth, 1922) of surface sediments in Lake Towuti is highly variable. Sand (63 to 2000 µm) ranges from 0.0 to 82.8% of the sediment and shows highest concentrations in the vicinity of large inlets, such as the Mahalona River, and generally higher values close to the shore (Fig. 5A). With increasing distance to the inlets and the shores, the sand content rapidly decreases. In the central part of the lake, sand is absent in 41 samples, but still accounts for 10.1% and 20.5% in samples 16 and 17 in the northernmost part of the lake, in 174.9 and 195.5 m water depths, respectively. Silt (2 to 63 µm) ranges from 11.9 to 75.9% and also shows highest concentrations in front of major inlets, in particular the Mahalona, Timampu, and Loeha rivers (Fig. 5B), but reaches its highest concentrations further away from the river inlets compared to the sand fraction. The clay fraction (<2 µm) varies between 3.4% and 71.8% and has highest concentrations in parts of the lake most distal from the inlets (Fig. 5C).

The sand, silt, and clay distributions are reflected by two distinct non-parametric EMs, which explain 85.4% of the variance in the grain-size data set and 93.7% of the median variance of the samples (Fig. 5D). One EM_{GS} represents the fine-grained fraction, with an average of 60.6% clay, 39.4% silt and no sand, whereas the other EM_{GS} is characteristic for the coarse-grained fraction with 13.2% clay, 57.9% silt and 28.9% sand.

The MS (0.7 to 10.4 x 10^{-6} kg/m^3) exhibits highest values at shallow, coastal sites along the eastern and southern shores, and in front of the Mahalona River (Fig. 5E). The MS values are positively correlated with the sand and silt contents (Fig. 5A and B).

Geochemistry

The TOC content (0.17 to 6.43%) is highest in the north-eastern and south-western areas of the lake, close to the shores but distant from the major inlets (Fig. 6A). The C/N ratio (4.5 to 24.0) is elevated in some near-shore areas, in particular in the north-eastern and eastern parts of the lake (Fig. 6B), which partly overlap with elevated TOC contents. The C/N values do not show a clear relationship with the locations of major inlets. A different pattern is shown by the $\delta^{13}C$ ratio (-37.45 to -32.18‰), which is characterized by distinctly heavier values in front of the Mahalona River (Fig. 6C).

The concentrations of Ti (0.03 to 0.41%), K (0 to 1.56%), Al (2.0 to 9.1%) and Si (7.1 to 19.6%) reach their highest values in front of the Loeha River (Fig. 6D to G). The Ti, K and Al concentrations remain high towards the deeper central part of the southern basin, whereas Si is slightly enriched in front of the Mahalona River in the north. Mg (2.3 to 18.5%) shows a strong maximum in front of the Mahalona River, as do Ca (0.27 to 5.31%) and Cr (0.12 to

>1%; Fig.6H to J). Ca and Cr have additional maxima in other near-shore areas, but at different location; Ca exhibits a pronounced maximum also in front of the Timampu inlets, while Cr is enriched in the southern and north-eastern lake parts. The distribution of Fe (6.5 to 28.9%) partly tracks that of Cr, with the most prominent enrichment occurring in the southern and north-eastern parts of the lake (Fig. 6K). Nevertheless, Fe shows a distinct minimum in front of the Mahalona River, where Cr concentrations are high. The distribution of Mn (0.06 to 0.56%) differs from all other elements, with maximum values in the north-eastern lake and in the central southern part of the lake, in front of the Larona outflow (Fig. 6L).

Mineralogy

Minerals of the serpentine group (including antigorite, nacrite, greenalite, lizardite and chrysotile) constitute 12.6 to 62.3% of the mineral assemblage and thus are the most abundant minerals in the surface sediments of Lake Towuti (Fig. 7A). This group has high concentrations over a large part of the lake but particularly in front of the Mahalona, Tomerakah and Taora rivers. This is due to maxima of antigorite (Fig. 7B) and nacrite (not shown) in these areas, which range from 5.5 to 48.2% and 5.7 to 17.7% in the sediments, respectively. A clearly different pattern is shown by the serpentine mineral greenalite, which reaches up to 16.0% in several samples from the southern basin of the lake, but is almost absent in the northern basin (Fig. 7C). Lizardite and chrysotile were only detected in few samples at low concentrations close to the detection limit of 5%.

The surface sediments contain significant amounts of four clay mineral groups: smectite, illite, chlorite and kaolinite. Smectite clays (including saponite, montmorillonite, vermiculite and other phases) constitute up to 46.4% of the minerals present (Fig. 7D). They are heterogeneously distributed, but with distinct minima for instance in front of the Timampu, Mahalona and Loeha rivers. Illite has a distinct maximum (with up to 61.8%) in front of the Timampu inlets (Fig. 7E). High concentrations also occur close to the Mahalona and Loeha rivers, and in south-western parts of the lake, including the area in front of the outflowing Larona River. Chlorites are also enriched in front of the Mahalona River, reaching maximum values of 17% (Fig. 7F). Except for this similarity, chlorite shows a distribution opposite to illite, with minima in front of the Timampu and Loeha rivers, and some enrichment in other near-shore areas. Compared to the other clay mineral groups, kaolinite shows a homogeneous distribution, comprising up to 22.9% of the sediment (Fig. 7G). The only exception is the area in front of the Mahalona River, which has significantly reduced kaolinite concentrations.

The distribution of quartz (2.5 to 45.0%, Fig. 7H) is characterized by a distinct maximum in front of the Loeha inlet and slightly enriched values in the north-western part of the lake, particularly in front of the Timampu inlets. A generally opposite pattern is shown by goethite, which constitutes up to 16.2% of the present minerals (Fig. 7I). Goethite shows highest concentrations in most of the southern lake basin and in the north-eastern region of the northern basin, and minima in front of the Timampu, Mahalona and Loeha rivers. The same minima are shown by the amphibole tremolite, which ranges from 7.3 to 54.2% (Fig. 7J). The amphibole hornblende was detected in only eight samples, located in front of the Timampu, Mahalona and Loeha rivers, with low concentrations of 3.6 to 5.9% (Fig. 7K). Additional minerals close to the detection limit of *ca* 5% are combined as ´others´ (Fig. 7L),

which constitute 7.5 to 21.4% of the present minerals. This group includes greenalite, magnetite, siderite, cuprite and spinel, also showing highest concentrations in front of the Timampu, Mahalona and Loeha rivers.

Tephra particles, mostly as glass shards, were found at low concentrations (<2.62 particles/1000) across the lake (Fig. 4C). Maxima occur south-east of the Mahalona River and, less pronounced, in other near-shore areas of the north-western (off the Timampu inlets), eastern (off the Tomerakah, Taora, and Loeha rivers), and southern lake (off the Tokolalo, Lantibu and Lengke rivers).

DISCUSSION

The physical, chemical, mineralogical and biological properties of the surface sediments from Lake Towuti show distinct spatial patterns (Figs 4 to 7) that reflect a variety of external and internal processes.

Sediment supply to the lake

SBecause it can be assumed that the dense vegetation in the catchment of Lake Towuti stabilizes the slopes and restricts aeolian sediment transport, the majority of allochthonous material supplied to the lake is likely to be of fluvial origin. This assumption is supported by strongly enriched sand and silt contents of the lake sediments in front of the major inlets, reaching values beyond those of other near-shore areas (Fig. 5). Furthermore, there is a generally good correspondence between the elemental compositions of these lake sediments

and those of the adjacent rivers in the different geologically distinct catchments (Figs 2 and 6; Costa et al., 2015;).

Statistical analysis of the geochemical data from the lake sediments identifies three major chemical end-members (Fig. 8): EM_{Chem} 1 is characterized by the highest Mg abundance, as well as relatively high Si scores, and is clearly elevated in front of the Mahalona River; EM_{Chem} 2 is characterized by the highest Si and Al scores and shows maxima in the northern part of Towuti's southern basin and, less pronounced, in the north-western part of the lake; and EM_{Chem} 3 is marked by a very high Fe score, and is highest in the southern and north-eastern parts of the lake. Merging these with mineralogical, sedimentological and biogeochemical datasets, summarized by an RDA (Fig. 9), a correlation matrix of all data (Fig. S1) and an end-member analysis of the mineralogical data (S2), five distinct fluvial sediment sources can be defined: (i) the Mahalona River to the north; (ii) the Timampu inlets to the north-west; (iii) the Loeha River to the east; (iv) the Lengke River to the south; and (v) the Lemo-Lemo River to the north-east of Lake Towuti (Fig. 2).

Mahalona River

The sediment deposited near the Mahalona River has elevated values of Mg and Si, and to a lesser extent Ca and Cr in front of the river delta (EM_{Chem} 1; Figs 8A and 9). High Mg concentrations (Fig. 6H) were also found in adjacent lake surface sediment samples by Weber et al. (2015) and in the Mahalona River itself by Costa et al. (2015) and Goudge et al. (2017). The enrichment of Mg can best be explained by an elevated supply of Mg-rich serpentines (Figs 7A and S2A), for example antigorite and lizardite. Antigorite shows a maximum in front of the Mahalona River (Fig. 7B) and is positively correlated with Mg ($r = 0.58$; Fig. S1). The Mg-end-member lizardite exclusively occurs in the same area, albeit with

low concentrations (therefore assigned to other minerals; Fig. 7L). Serpentines are minerals derived from the surrounding ophiolites (Fig. 2); they are either formed during serpentinization on the deep-sea floor through hydrothermal alteration of mafic and ultramafic rocks prior to their uplift to form the island of Sulawesi, or in the case of lizardite, occur as a secondary mineral provided by chemical weathering in the saprolite zone (Apostolidis and Distin, 1978). Another potential source of Mg could be chlorites, detected in small amounts in the serpentinized peridotites to the north of Lake Towuti. Chlorites have generally lower concentrations in Lake Towuti, but do have a distinct maximum in front of the Mahalona River (Figs 7F and S2A).

The relatively high Si concentrations in front of the Mahalona River (Fig. 6G) may be explained by fluvial input of silicates, including the serpentine minerals antigorite (Fig. 7A) and lizardite; the illite clay mineral group (Fig. 7E) and the chlorite clay mineral group (Fig. 7F), as well as hornblende (Fig. 7K). Additional supply may originate from quartz veins, which were observed in the saprolite and laterite horizons of soil profiles to the north of Lake Towuti (Silver et al., 1983). Furthermore, the Si distribution shows a similar pattern to that of tephra particles (Fig. 4C), which likely originate from volcanoes located in North Sulawesi (Wilson and Moss, 1999). The tephra particles are enriched in the surface sediments in front of the major inlets, suggesting fluvial remobilization from the catchment. The highest concentrations in front of the Mahalona River might be due to successive remobilization from the Quaternary alluvium making up most of the catchment of the Lampensiu River, a tributary of the Mahalona River (Figs 1 and 2), where volcanic ash from several eruptions could have accumulated.

In contrast to Mg and Si, the enrichment of Ca in front and west of the Mahalona Delta (up to 5.31%; Fig. 6I) cannot exclusively be traced back to supply from the Mahalona River. This is indicated by the Ca concentration in the Mahalona River sediment, which average 1.31% (Costa et al., 2015), thereby being higher than in many of the rivers entering Lake Towuti, but lower than the concentrations observed in the lake sediment in this region (Fig. 7A). Hence, the Ca enrichment cannot be explained by fluvial supply from the Mahalona River alone but needs additional sources. The most likely source is *in situ* production from calcareous macrofossils, such as molluscs. Molluscs are not present in the Mahalona River but were found in shallow waters of Lake Towuti (<4.5 m water depth), for instance at sample location 18 directly in front of the Mahalona Delta (Table 1; Fig. 1).

The Cr enrichment in front of the Mahalona Delta (up to >1%; Fig. 6J) also cannot solely be explained by fluvial supply, since the Cr concentrations in the Mahalona River sediments (0.93%) are lower than the average values of the rivers entering the lake (1.35%; Costa et al., 2015). The Cr predominantly derives from Cr-spinels, including chromite, which originate from the ultramafic and mafic catchment rocks and are included in the group of 'other minerals' (Fig. 7L). Chromium-spinels have been detected by EDX analysis on thin sections in the basal, sandy parts of turbidites occurring in a piston core (Co1230) taken in front of the Mahalona Delta (Vogel et al., 2015). Spinels observed in the smear slides of Lake Towuti´s sediments are quite large and almost euhedral mineral grains. Their presence in surface sediments in front of the Mahalona Delta is confirmed by EDX analyses. Because the observed high Cr values generally occur in coarser-grained, sandy sediments (Fig. 5A), the concentrations of Cr-spinels may be enriched by shallow-water winnowing leading to particle-size sorting.

Another potential source of Cr in front of the Mahalona River could be mining and smelting. Mining and smelting has taken place since 1968 to the north of Lake Towuti, in the catchments of Lake Matano and Lake Mahalona (Fig. 2) and thus could have significantly changed the composition of the surface sediment samples. However, since samples from this study integrate *ca* 200 to 250 years, any anthropogenic Cr pollution would have occurred during only 25% of this time and thus would significantly be diluted. In any case a significant contamination of Cr from the mines and smelters is highly unlikely. First, the Cr concentrations in the lake surface and river sediments argue against a significantly increased fluvial supply via the Mahalona River; in fact, the highest Cr concentrations occur in the Lengke, Lantibu and Tokolalo inlets (1.00 to 2.38%; Costa et al., 2015), furthest from the mine smelter. Second, an aeolian supply would have led to a Cr enrichment in particular in the lake centre via atmospheric deposition of fine particles followed by shallow-water winnowing; however, the Cr concentrations are lowest in the centre of the lake (<1200 ppm). Third, the Cr concentrations in the surface sediments close to TDP Site 1 (Fig. 1) are comparable to the Holocene samples of a sediment core from the same area (Costa et al., 2015), which represent the geogenic background. This also suggests that contamination by Fe from mining and smelting can be excluded, since Fe shows particularly low concentrations in front of the Mahalona River and in the central lake basin.

Loeha and Timampu Rivers

End-member$_{Chem}$ 2 is reflected by high amounts of Si, Ca, Ti, K and Al (Figs 8B and 9) and shows the strongest maximum offshore from the Loeha and Bantilang rivers along the eastern shore in the southern part of the lake (Fig. 6D to G and I). A secondary maximum of EM$_{Chem}$ 2 occurs in the north-western corner of the lake, offshore from the Timampu inlets. Slightly higher Si concentrations in front of the Timampu and Loeha rivers than in front of the

Mahalona River (see above) suggest additional Si supply from the sandstones and siltstones occurring in the Wasuponda Mélange to the north-west and from the metasediments exposed to the east of Lake Towuti, respectively (Fig. 2).

Elevated Ca concentrations in front of the Timampu and Loeha rivers may partially be explained by *in situ* production from calcareous macrofossils, which for instance occur at sampling sites 2 and 5 close to the shore off the Timampu inlets (Table 1; Fig. 1). Additional sources for the Loeha River may be Ca-bearing minerals in the metasediments, which are exposed in the Loeha catchment (Fig. 2). Even higher Ca concentrations in front of the Timampu inlets argue for additional sources in the undefined ultramafic rocks that are widespread in the Timampu catchment (Fig. 2). In addition, Ca supply from restricted limestone outcrops, which are known to occur in wider areas to the west of the Timampu catchment, cannot be excluded.

In contrast to Si and Ca, the enrichments of Ti, K and Al in front of the Loeha River, as well as of Ti and Al in front of the Timampu inlets, differ strongly from minimum values of these elements in the sediments in front of the Mahalona River (Fig. 6D to F). The enriched Ti content in front of the Loeha River is in agreement with elevated Ti concentrations in the river itself (Costa et al., 2015). Elevated Al content in the north-western part of the lake was also observed by Weber et al. (2015). The Ti enrichment, as well as that of K and Al, in the Loeha River is probably derived from the felsic metasediments occurring in the catchment (Fig. 2). Elevated Ti and Al concentrations in front of the Timampu inlets, corresponding with a depletion in K, are potentially due to significant sediment supply from the sandstones and siltstones in the Wasuponda Mélange to the northwest of Lake Towuti (Fig. 2). The sediment supply obviously includes illite (Fig. 7E) and kaolinite (Fig. 7G),

which may result from intense weathering of silicates. Kaolinite may additionally originate from the laterite soils formed on top of serpentinized and unserpentinized bedrock in the catchment.

Lengke and Lemo-Lemo rivers

High score percentages of EM_{Chem} 3 occur in the southern and north-eastern parts of Lake Towuti, in front of the Lengke and Lemo-Lemo rivers, respectively (Figs 8C and 9); they mainly reflect very high Fe concentrations (Fig. 6K), and are also characterized by elevated Cr (Fig. 6J) and Ni concentrations. High Fe and Cr concentrations were also reported by Costa et al. (2015) from sediment samples off of river mouths at the southern shore.

Iron enrichment can predominantly be related to supply from the saprolites and laterites that are formed on top of the peridotites in the catchment (Fig. 2) and are characterized by Fe concentrations of up to 49%. The Fe oxyhydroxide goethite is the dominant mineral phase of these Fe oxides. This corresponds well with positive correlations of the EM_{Chem} 3 scores with goethite ($r = 0.72$; Fig. S1) and Fe concentrations ($r = 0.69$; Fig. S1). Another mineral likely to contribute to the Fe enrichment in the sediments is magnetite. Magnetite has been detected with less than 5% abundance in the surface sediments (therefore assigned to other minerals; Fig. 7L). It may be supplied to the lake from the catchment, where it was found to be enriched in the coarse fraction of the laterites and detected as an accessory mineral in the peridotite rocks. Magnetite is also produced in the water column of Lake Towuti (Tamuntuan et al., 2015; Vuillemin et al., 2016). In the southern lake area, additional Fe supply is likely derived from greenalite, the Fe-enriched form of the serpentine group, a common mineral phase in the serpentinized ultramafic bedrock that reaches concentrations of up to 16.1% (sample 68) in the surface sediments (Fig. 7C).

The elevated concentrations of Cr and Ni in the lake surface sediments can also be traced back to supply from the saprolite and laterite horizons in the catchment. There, they are enriched by secondary serpentinization at the bedrock–soil interface. In addition, weathering of Cr-spinels releases Cr and Ni, which can be incorporated into silicates such as kaolinite (Fig. 7G; Koppelman et al., 1980; Jiang et al., 2010). Chromium may also be incorporated into goethite (Fig. 7I), as suggested by a distinct positive correlation ($r = 0.62$; Fig. S1).

Steep catchment slopes

While the abundances of EM_{Chem} 1 and EM_{Chem} 2 appear to reflect distinct fluvial sediment sources, EM_{Chem} 3 may also be influenced by shoreline and catchment morphologies. The highest EM_{Chem} 3 scores occur in front of the south-western and northeastern shores, where the slopes at the shoreline are particularly steep (Fig. 1). Hence, the adjacent lake sediments could be influenced not only by fluvial sediment supply but also by mass wasting and direct run-off from the slopes (e.g. Vogel et al., 2015). These processes may have intensified recently due to increased deforestation in the catchment of Lake Towuti (Nasution, 2007), driven by manual wood factories and regional population growth, as well as the expansion of the agriculture area per farmer (Dechert et al., 2004). Deforestation could have increased the vulnerability of the slopes to mass wasting and run-off, possibly, but not exclusively, in combination with high seismic activity.

When mass movement and run-off events occur, they can enter the lake, spreading fine-grained material from the laterites far into the lake, as indicated by the broad distribution of the clay fraction (Fig. 5C). Together with high contents of the particularly fine-grained

clay mineral group smectite (Fig. 7D), this suggests a low-energy setting, with limited fluvial supply to the distal lake areas.

Lake-internal physical and chemical processes

The highest transport energies in Lake Towuti, as indicated by increased sand and silt content, occur in front of major inlets, in shallow waters along the lake shores, and in areas influenced by subaquatic mass movement processes (Fig. 5A and B).

The sediments directly in front of the inlets often show enriched sand content (Fig. 5A). Further offshore, the sediments are characterized by high silt content, in particular in front of the Mahalona, Timampu and Loeha rivers (Fig. 5B). This reflects successive deposition from suspension and hydrodynamic sorting with distance from the inlet. The extension of the silt enrichment relatively far into the lake suggests that the distribution is also influenced by hyperpycnal flows or by wave-driven sediment resuspension and focusing from the river mouths to the deeper lake areas.

High sand content also characterizes the lake areas close to the shorelines in between some of the inlets (Fig. 5A), in particular at sampling sites with distances of less than 1 km from the shore. These areas differ from those adjacent to steep slopes, thus excluding an impact of terrestrial mass movement and rather suggesting shoreline erosion, resuspension and lateral sediment transport along the lake shores, presumably by wave action.

Recent subaquatic mass movements are indicated in the northern part of Lake Towuti, close to TDP Site 2 (Fig. 1). There, the surface sediments have sand contents of 10.1%, 20.5% and 3.2% at sampling locations 16, 17 and 22, respectively, in water depths between 171.4 m and 195.5 m, and at distances between 2.8 km and 4.5 km to the shore (Fig. 1). The position of this sand enrichment can neither be explained by fluvial supply nor by near-shore redeposition, so it most likely results from deposition by lateral transport via mass movement events. This suggestion is supported by the appearance of terrestrial macrofossils at all three locations, since macrofossils otherwise are enriched in near-shore samples only (Table 1). Furthermore, sample 16 exhibits a characteristic bimodal grain-size distribution, which according to Vogel et al. (2015) is an indicator for increased sediment input from hyperpycnal flows in deeper, distal parts of Lake Towuti. The composition of the mass movement deposits suggests sourcing from the Mahalona Delta slopes at the northern shore. Without having detailed information on the structure of the delta, it is inferred that these mass movement deposits are turbidites. The occurrence of at least one turbidite in the surface sediments, which were deposited during the past *ca* 200 to 250 years, is not surprising, taking the mean turbidite recurrence rate of *ca* 300 years identified by Vogel et al. (2015) in a 19.8 m long sediment core covering the last *ca* 30 000 years close to TDP Site 2 in the same area (Fig. 1).

Furthermore, the composition of the surface sediments argues for at least occasional oxygenation of the entire water column. For instance, both the Fe and Mn distributions are highly heterogeneous and do not show systematically lower concentrations in deeper water that might be expected from reductive Fe dissolution of oxides under anoxic conditions (Fig. 6K and 6L; Davison 1993; Kylander et al., 2011). Although low Mn and Fe values in the northern basin could result from the absence of oxygen, much higher values in the southern

basin, reaching water depths of 160 m, clearly argue against permanently anoxic conditions. Much of this iron could reside in silicates or other minerals that are not susceptible to reductive dissolution. However, the distribution of the Fe oxyhydroxide goethite, which has a high concentration in the southern basin (Fig. 7I), also argues against permanent anoxia. Measurements of temperature, oxygen and dissolved iron concentration in the upper 140 m of Lake Towuti's water column, conducted between September 1995 and June 2015 (Costa et al., 2015; Vuillemin et al., 2016), suggest that Lake Towuti usually does not mix to the bottom and is oxygen depleted in water depths below *ca* 100 m.

Biogenic sedimentation

Total organic carbon is concentrated in the south-western and north-eastern parts of Lake Towuti (Fig. 6A), in areas close to steep catchment slopes and distant to major inflows (Fig. 1), and where fine-grained deposition prevails (Fig. 5C). The C/N ratio in the surface sediments averages 10.8, arguing for a predominance of autochthonous biogenic production. These values slightly exceed traditional end-member values for aquatic OM, but given Lake Towuti's N-poor, ultra-oligotrophic status in combination with water temperatures of *ca* 28°C and occasional mixing of the water column, these C/N ratios at least partly result from substantial lake-internal nitrogen recycling (Talbot et al., 2006). Intermixing with allochthonous OM sources is indicated by elevated C/N ratios in front of the Mahalona and Loeha inlets, and in front of the steep slopes at the northeastern shore, suggesting fluvial and gravitational supply. This is partly supported by terrestrial macrofossil remains, such as leaves, rods and twigs, which mainly occur in near-shore samples, but also distal areas in front of the Mahalona River (Table 1). Allochthonous OM supply via the Mahalona River is furthermore indicated by a distinct trend towards heavier $\delta^{13}C_{OM}$ values in the northern lake

part (Fig. 6C). Potentially, this trend reflects stronger supply of terrestrial OM originating from tropical grasses (C4 plants; Meyers and Lallier-Vergès, 1999), which are widespread in the plain terrain of the Mahalona River. However, samples with elevated $\delta^{13}C_{OM}$ values do not have higher C/N ratios, suggesting low terrigenous OM contributions. Alternatively, autochthonous OM can obtain a terrigenous $\delta^{13}C_{OM}$ value while maintaining low C/N ratios due to algal and microbial metabolism of terrestrially-sourced dissolved inorganic and organic carbon (Webb et al., 2016). Data from this study suggests that this may occur on a catchment scale in Lake Towuti.

Additional indicators of autochthonous biological production in Lake Towuti are calcareous shells, which mainly occur in near-shore samples (3, 12, 25, 32, 73, 74 and 79; Fig. 1), and sponge spicules and diatoms (Fig. 3). The sponge spicules are enriched in near-shore areas, in front of some minor inlets (Fig. 4B). This suggests that the sponges prefer locations with mildly turbid waters and low sedimentation rates, which provide nutrients but do not result in burial of the filter-feeding organisms. The proximity to the inlets may be of importance for nutrient supply, including Si, given the ultra-oligotrophic status of the lake. The distribution of diatoms in the surface sediments is similar to that of the sponge spicules (Fig. 4A). The diatoms may be partly dependent on the nutrient supply by the inlets; however, since the majority of the diatoms in Lake Towuti are benthic, they likely derive the Si and P required for their growth from sediment reflux. If so, the distribution of the benthic diatoms is mainly supported by shallow and clear waters, with sufficient light available (modern Secchi depth is 22 m, therefore light transparency is *ca* 40 m; Lehmuslouto et al., 1995; von Rintelen et al., 2012).

Based on the TOC contents, C/N ratios, $\delta^{13}C_{OM}$ values, and concentrations of calcareous shells, sponge spicules and diatoms in the surface sediments, the biogenic sedimentation in Lake Towuti is predominantly controlled by natural processes. Except for the potential impact of deforestation in the north-eastern and south-western lake catchments, which could lead to enhanced TOC supply via mass wasting and direct run-off, an anthropogenic impact is not discernible in data from this study. This includes the lack of evidence for increased primary production due to nutrient supply in front of major settlements (*cf*. Fig. 2).

Implications for the palaeorecord

The understanding gained from the here presented study of surface sediments concerning the modern processes operating in Lake Towuti has a number of implications for similarly structured research projects on large tropical lakes and, in this case, also for ongoing palaeoenvironmental investigation of the TDP drill cores (Fig. 1). These sediment cores predominantly consist of pelagic clays, which are interrupted by turbidites, tephra layers, diatomaceous oozes, and, at the base of the core, a variety of shallow-water and fluvial deposits, such as peats, gravels and sands (Russell et al., 2016).

This study of modern lake sediments provides a detailed characterization of the chemical, sedimentological and biological signature of fluvial and other sediment sources. It will facilitate disentangling the changing influence of different sediment sources in the palaeorecord of this complex tropical setting. The pelagic sediments in Lake Towuti today are predominantly of fluvial origin, with chemical and mineralogical compositions characteristic of five distinct source areas. This finding will enable researchers to relate

changes in fluvial sediment supply in the palaeorecord to environmental processes, in particular tectonic activity, lake-level fluctuations and changes in the hydrological connectivity of lakes Towuti, Mahalona and Matano (Fig. 1; Russell et al., 2016). As suggested by investigations in the catchment of Lake Towuti, the kaolinite content in the pelagic sediments may reflect the degree of chemical weathering. In contrast, the current study has revealed that classical proxies for lake mixing behavior, such as the concentrations of redox-sensitive elements (for example, Fe, Mn and Cr), siderite and vivianite (Melles et al., 2012; Vuillemin et al., 2017), do not unequivocally reflect anoxia and thus have to be interpreted with caution in ancient sediments of Lake Towuti.

In short sediment records from Lake Towuti, turbidity currents have been identified as an important sedimentation process (Vogel et al., 2015). The sub-recent turbidite identified in this study in the northern basin of Lake Towuti differs from the pelagic sediments by the occurrences of coarser grains, terrestrial OM and shallow-water calcareous macrofossils. This composition indicates that the turbidites can remobilize and transport shallow-water sediments into the deep lake basin. With the multi-disciplinary characterization of the various shallow-water areas in modern Lake Towuti, potentially different sources of turbidites in the palaeorecord may be attributed to specific source areas in the lake. This, in turn, could be indicative of areal changes in sediment supply and tectonic activity through time. Furthermore, variations in the frequency and thickness of turbidites may be traced back to changes in earthquake activity, lake-level, precipitation and vegetation.

Tephra occurs in the surface sediments of Lake Towuti as dispersed particles with characteristic grain shapes but not as distinct layers. This indicates that presently, tephra particles are predominantly remobilized and supplied by fluvial activity from the catchment.

In the palaeorecord, tephra may thus occur both as a product of direct fallout and as a more diffuse signal of remobilized particles from the catchment. Direct fallout may be differentiated from redeposited tephra by sharper shard edges. Remobilization of the tephra deposited in the catchment can increase the supply of Si and other elements to the lake for a longer period of time. This tephra supply may have played an important role for the degree of biogenic production by diatoms and sponges, taking its high Si content and the ultra-oligotrophic, Si-limited nature of the lake. Diatoms and sponge spicules are rare in the surface sediments, but occur close to areas with higher concentrations of tephra particles in the surface sediments.

The shallow-water surface sediment samples are composed of rather coarse-grained deposits with high MS values and Cr concentrations; they exclude peat and differ from all other deposits mainly by the occurrence of diatom frustules and sponge spicules. Hence, coarse-grained deposits with comparable compositions occurring in the TDP cores can be traced back to shallow-water environments at the coring site during the time of deposition, or to extensive redeposition of the sediments. The occurrence of peat layers and fluvial sediments, in contrast, represent times, when no lake existed at the drill sites.

CONCLUSION

A multi-proxy approach combining sedimentological, geochemical, mineralogical and microscopic analyses with statistical methods was performed on a set of 84 surface sediment samples from Lake Towuti, Indonesia. The results provide a detailed understanding of the major physical, chemical and biological processes controlling modern sedimentation in this tropical lake. These results will facilitate the reconstruction of the climatic and environmental

history based upon the composition of Towuti Drilling Project (TDP) drill cores recovered in 2015.

The composition of the surface sediments in Lake Towuti is highly heterogeneous. Sedimentation is controlled mainly by fluvial sediment supply from five distinct source areas. The individual chemical and mineralogical signatures can be traced relatively far into the lake. Near-shore environments are additionally influenced by redeposition due to wave action. Most calm settings, with deposition of fine-grained particles and organic matter (OM), occur in the central lake, most distal to the major inlets. There, coarser grain sizes are related to aquatic mass movement events that ignite hyperpycnal flows. Biogenic silica derived from diatoms and sponges is found only in special ecological niches, which are dependent on individual water depths, light availabilities, nutrients and the degree of turbidity.

Significant anthropogenic impacts on the composition of the surface sediment samples, which average the sedimentation over the past *ca* 200 to 250 years, is not evident from the data in this study. However, mass wasting and direct run-off on the steep north-eastern and south-western catchment slopes may have become amplified by deforestation. In contrast, Cr and Fe supply from mines and smelters to the north of Lake Towuti is not yet reflected in the chemistry of the surface sediments. The same holds true for human impact on the amount of biogenic accumulation, which seems to be unaffected by influences from nearby settlements.

In interpretation of the TDP cores, attribution of chemical and mineralogical proxies to different sediment source areas is of special importance. Based on measurements of the respective indicators in the pelagic sediments and mass movement deposits in the drill cores, the individual source areas may be reconstructed. This will help with understanding changes in palaeogeography, for example in the hydrological connectivity between the Malili Lakes through the Mahalona River (Fig. 1), which could be controlled by climatic variations within the Indo-Pacific Warm Pool (IPWP) region as well as tectonic activity. Taking the environmental limitations of diatoms and sponges today, investigations of siliceous microfossils in the TDP cores may contribute to the understanding of lake-level changes, which could be triggered by orbital-scale climate changes and/or short-term El Niño–Southern Oscillation (ENSO) events. Furthermore, they may help to reconstruct the nutrient availability in the water column, which is dependent, for instance, on the weathering conditions in the catchment, on volcanic ash supply and on lake-internal mixing.

Towuti Drilling Project Sites 1 and 3 are located in an area (Fig. 1) which is dominated by pelagic sedimentation and may be influenced by all three chemically and mineralogically distinct sediment sources (EM_{Chem} 1 to 3 and EM_{Min} 1 to 3; Figs 8 and S2). This makes them ideal sites for reconstruction of the regional environmental and climatic history. In contrast, the upper 62 m of TDP Site 2, is mainly built up of mass movement deposits, intercalated with pelagic sediments and, in the present, is primarily influenced by only two major sources, reflected by EM_{Chem} 1 and 3 (Fig. 8) as well as EM_{Min} 1 and 3 (Fig. S2). This supports the use of TDP Site 2 for the reconstruction of the fluvial input and mass movement history in the northern basin of Lake Towuti, which may mainly mirror the history of the Mahalona River and the lakes further upstream, but also reflect lake-level fluctuations and seismic events.

ACKNOWLEDGEMENTS

The Towuti Drilling Project was partially supported by grants from the International Continental Scientific Drilling Program (ICDP), the US National Science Foundation (NSF), the German Research Foundation (DFG, grant no. ME 1169/26), the Swiss National Science Foundation (SNSF; 20FI21_153054/1 and 200021_153053/1), Brown University, Genome British Columbia, and the Ministry of Research, Technology and Higher Education (RISTEK). PT Vale Indonesia, the US Continental Drilling Coordination Office, the GeoForschungsZentrum Potsdam, and DOSECC Exploration Services are acknowledged for the logistical assistance to the project. This research was carried out with permission from RISTEK, the Ministry of Trade of the Government of Indonesia, the Natural Resources Conservation Center (BKSDA), and the Government of Luwu Timur of Sulawesi. We like to thank Hannah Jauss, University of Cologne, for her competent help in the FlowCam analyses. Special thanks are due to Paul Hamilton for the diatom identification and information about their preferred living conditions, to Doug Haffner for providing unpublished chemical data of the water column, and to Rachel Sheppard for providing unpublished mineralogical and spectroscopically data of the surface sediment samples. We are also grateful to two anonymous reviewers and editors Peir Pufahl and Ola Kwiecien for their comments and suggestions, which greatly helped to improve the manuscript.

REFERENCES

Aldrian, E. and Dwi Susanto, R. (2003) Identification of three dominant rainfall regions within Indonesia and their relationship to sea surface temperature. *Int. J. Climatol.*, **23**, 1435-1452.

Apostolidis, C.I. and Distin, P.A. (1978) The kinetics of the sulphuric acid leaching of nickel and magnesium from reduction roasted serpentine. *Hydrometallurgy,* **3**, 181-196.

Bramburger, A.J., Hamilton, P.B. and Haffner, G.D. (2014) Effects of a simulated upwelling event on the littoral epilithic diatom community of an ancient tropical lake (Lake Matano, Sulawesi Island, Indonesia). *Hydrobiologia*, **739**, 133-143.

Chiang, J.C.H. (2009) The Tropics in Paleoclimate. *Annu. Rev. Earth Planet. Sci.*, **37**, 263-297.

Chen, D. and Cane, M.A. (2008) El Niño prediction and predictability. *J Comput Physics*, **227**, 3625-3640.

Clement, A.C., Cane, M.A. and Seager, R. (2001) An orbitally driven tropical source for abrupt climate change. *J. Climate*, **14**, 2369-2375.

Coelho, A.A. (2003) Indexing of powder diffraction patterns by iterative use of singular value decomposition. *J. Appl. Crystallogr.*, **36**, 86-95.

Costa, K.M., Russell, J.M., Vogel, H. and Bijaksana, S. (2015) Hydrological connectivity and mixing of Lake Towuti, Indonesia in response to paleoclimatic changes over the last 60,000 years. *Palaeogeogr. Palaeoclimatol. Palaeoecol.,* **417**, 467-475.

Davison, W. (1993) Iron and manganese in lakes. *Earth-Sci. Rev.*, **34**, 119-163.

Dechert, G., Veldkamp, E. and Anas, I. (2004) Is soil degradation unrelated to deforestation? Examining soil parameters of land use systems in upland Central Sulawesi, Indonesia. *Plant and Soil*, **265**, 197-209.

Francke, A., Wennrich, V., Sauerbrey, M., Juschus, O., Melles, M. and Brigham-Grette, J. (2013) Multivariate statistic and time series analyses of grain-size data in Quaternary sediments of Lake El'gygytgyn, NE Russia. *Clim. Past*, **9**, 2459-2470.

Golightly, P.J. and Arancibia, O.N. (1979) The chemical compostion and infrared spectrum of nickel-and iron-substituted serpentine from a nickeliferous laterite profile-Soroako-Indonesia. *Can. Mineral.*, **17**, 719-728.

Goudge, T.A., Russell, J.M., Mustard, J.F., Head, J.W. and Bijaksana S. (2017) A 40,000 yr record of clay mineralogy at Lake Towuti, Indonesia: Paleoclimate reconstruction from reflectance spectroscopy and perspectives on paleolakes on Mars. *Geol. Soc. Am. Bull.*, B31569-1.

Haffner, G.D., Hehanussa, P.E. and Hartoto, D. (2001) The biology and physical processes of large lakes of Indonesia: Lakes Matano and Towuti. In: *The Great Lakes of the*

World: *Food-web, Health and Integrity* (Eds **M. Munawar** and **R.E. Hecky**), pp. 183-192. Backhuys Publishers, Leiden.

Hamilton, W.B. (1979) Tectonics of the Indonesian region (Geol Surv Profess Paper 1078). *US Govt. Print. Off.*, 308 pp.

Hecky, R.E., Campbell, P. and Hendzel, L.L. (1993) The stoichiometry of carbon, nitrogen, and phosphorus in particulate matter of lakes and oceans. *Limnology and Oceanography*, **38**, 709-724.

Hendon, H.H. (2003) Indonesian Rainfall Variability: Impacts of ENSO and Local Air-Sea Interaction. *J. Climate*, **16**, 1775-1790.

Heslop, D. and Dillon,M. (2007) Unmixing magnetic remanence curves without a priori knowledge. *Geophys. J. Intern.*, **170**, 556-566.

Jiang, M.Q., Jin, X.Y., Lu, X.Q. and Chen, Z.L. (2010) Adsorption of Pb (II), Cd (II), Ni (II) and Cu (II) onto natural kaolinite clay. *Desalination*, **252**, 33-39.

Kadarusman, A., Miyashita, S., Maruyama, S., Parkinson, C.D. and Ishikawa, A. (2004) Petrology, geochemistry and paleogeographic reconstruction of the East Sulawesi Ophiolite, Indonesia. *Tectonophysics*, **392**, 55-83.

Konecky, B., Russell, J. and Bijaksana, S. (2016) Glacial aridity in central Indonesia coeval with intensified monsoon circulation. *Earth-Planet Sci. Lett.*, **437**, 15-24.

Koppelman, M.H., Emerson, A.B. and Dillard, J.G. (1980) Adsorbed Cr (III) on chlorite, illite and kaolinite - an X-ray photoelectron spectroscopic study. *Clay and Clay Minerals*, **28**, 119-124.

Kylander, M.E., Ampel, L., Wohlfarth, B. and Veres, D. (2011) High-resolution X-ray fluorescence core scanning analysis of Les Echets (France) sedimentary sequence: new insights from chemical proxies. *J. Quatern. Sci.*, **26**, 109-117.

Lehmusluoto, P., Machbub, B., Terangna, N., Rusmiputro, S., Achmad, F., Boer, L., Brahmana, S.S., Priadi, B., Setiadji, B., Sayuman, O. and Margana, A. (1995) National Inventory of the Major Lakes and Reservoirs in Indonesia. Expedition Indodanau Technical Report, Edita Oy, Helsinki, 71 pp.

Melles, M., Brigham-Grette, J., Minyuk, P.S., Nowaczyk, N.R., Wennrich, V., DeConto, R.M., Anderson, P.M., Andreev, A.A., Coletti, A., Cook, T.L., Haltia-Hovi, E., Kukkonen, M., Lozhkin, A.V., Rosén, P., Tarasov, P., Vogel, H. and Wagner, B. (2012) 2.8 million years of Arctic climate change from Lake El'gygytgyn, NE Russia. *Science*, **337, 315-320.**

Meyers, P.A. and Lallier-Vergès, B.J. (1999) Lacustrine sedimentary organic matter records of Late Quaternary paleoclimates. *Journal of Paleolimnology*, **21**, 345-372.

Monnier, C., Girardeau, J., Maury, R.C. and Cotton, J. (1995) Back-arc basin origin for the East Sulawesi ophiolite (eastern Indonesia). *Geology*, **23**, 851-854.

Morlock, M.A., Vogel, H., Nigg, V., Ordoñez, L., Hasberg, A.K.M., Melles, M., Russell, J.M., Bijaksana, S., TDP Science Team (submitted): Climatic and tectonic controls on source-to-sink processes through space and time in a tropical ultramafic lake catchment: Lake Towuti, Indonesia. *Earth Surface Processes and Landforms*

Nasution, **S.H.**, (2007) Growth and condition factor of Rainbow Selebensis (Telmatherina celebensis Boulenger) in Lake Towuti, South Sulawesi. *Ind. Fish. Res. J.*, **13**, 117-123.

Pierrehumbert, R.T. (1999) Subtropical water vapor as a mediator of rapid global climate change. In: *Mechanisms of Global Climate Change at Millennial Time Scales* (Eds **P.U. Clark, R.S. Webb** and **L.D. Keigwin**), American Geophys. Union, Geog. Monogr., 112, 1-35.

PT Vale (2017) vale.com/indonesia/EM/aboutvale/history/pages/default.aspx

Robinson, K.M. (1986) *Stepchildren or Progress - The Political Economy of Development in an Indonesian Mining Town.* SUNY Press, *Albany*, New York, 323 pp.

Roy, D., Paterson, G., Hamilton, P.B., Heath, D.D. and Haffner, G.D. (2007) Resource-based adaptive divergence in the freshwater fish Telmatherina from Lake Matano, Indonesia. *Molecular Ecology*, **16**, 35-48.

Russell, J.M., Bijaksana, S., Vogel, H., Melles, M., Kallmeyer, J., Ariztegui, D., Crowe, S., Fajar, S., Hafidz, A., Haffner, D., Hasberg, A., Ivory, S., Kelly, C., King, J., Kirana,

K., Morlock, M., Noren, A., Grady, R., Ordonez, L., Stevenson, J., von Rintelen, T., Vuillemin, A., Watkinson, I., Wattrus, N., Wicaksono, S., Wonik, T., Bauer, K., Deino, A., Friese, A., Henny, C., Imran, Marwoto, R., Ngkoimani, L.O., Nomosatryo, S., Safiuddin, L.O., Simister, R., Tamuntuan, G. (2016) The Towuti Drilling Project: paleoenvironments, biological evolution, and geomicrobiology of a tropical Pacific lake. *Scientific Drilling*, **21**, 29-40.

Russell, J.M., Vogel, H., Konecky, B.L.K., Bijaksana, S., Yongsong, H., Melles, M., Wattrus, N., Costa, K. and King, J. (2014) Glacial forcing of central Indonesian hydroclimate since 60,000 y B.P. *PNAS*, **111**, 5100-5105.

Sabo, E., Roy, D., Hamilton, P.B., Hehanussa, P.E., McNeely, R. and Haffner, G.D. (2008) The plankton community of Lake Matano: factors regulating plankton composition and relative abundance in an ancient, tropical lake of Indonesia. *Hydrobiologia*, **615**, 225-235.

Scott, P. (1983) The Geometries of 3Manifolds. Bulletin of the London Mathematical Society**, 15, 401-487**.

Spakman, W. and Hall, R. (2010) Surface deformation and slab–mantle interaction during Banda arc subduction rollback. *Nature Geoscience*, **3**, 562-566.

Silver, E.A., McCaffrey, R. and Smith, R.B. (1983) Collision, rotation, and the initiation of subduction in the evolution of Sulawesi, Indonesia. *J. Geophys. Res.*: *Solid Earth*, **88**, 9407-9418.

Środoń, J., Drits, V.A., McCarty, D.K., Hsieh, J.C. and Eberl, D.D. (2001) Quantitative X-ray diffraction analysis of clay-bearing rocks from random preparations. *Clay Clay Mineral.*, **49**, 514-528.

Talbot, M.R., Jensen, N.B., Lærdal, T. and Filippi, M.L. (2006) Geochemical responses to a major transgression in giant African lakes. *Journal of Paleolimnology*, **35**, 467-489.

Tamuntuan, P., Bijaksana, S., King, J., Russell, J., Fauzi, U., Maryunani, K. and Aufa, N. (2015) Variation of magnetic properties in sediments from Lake Towuti, Indonesia, and its paleoclimatic significance. *Palaeogeography, Palaeoclimatology, Palaeoecology*, **420**, 163-172.

Tauhid, Y.I. and Arifian, J. (2000) Pengamatan Jangka Panjang Kondisi Air Danau Towuti. *Jurnal Sains and Teknologi Modifikasi Cuaca*, **1**, 91-100.

Udden, J.A. (1914). Mechanical composition of clastic sediments. *Geol. Soc. Am. Bull.*, **25**, 655-744.

Vaillant, J.J., Haffner, G.D. and Cristescu, M.E. (2011) The ancient lakes of Indonesia: towards integrated research on speciation. *Integrative and Comparative Biology*, **51**, 634-643.

Vogel, H., Wessels, M., Albrecht, C., Stich, H.B. and Wagner, B. (2010) Spatial variability of recent sedimentation in Lake Ohrid (Albania/Macedonia). *Biogeosciences*, **7**, 3333-3342

Vogel, H., Russell, J.M., Cahyarini, S.Y., Bijaksana, S., Wattrus, N., Rethemeyer, J. and Melles, M. (2015) Depositional modes and lake-level variability at Lake Towuti, Indonesia, during the past ~29 kyr BP. *J. Paleolimnol.*, **54**, 359-377

Vogt, C., Lauterjung, J. and Fischer, R.X. (2002) Investigation of the clay fraction (<2µm) of the clay minerals society reference clays. *Clay Clay Mineral.*, **50**, 388-400.

von Rintelen, T., von Rintelen, K., Glaubrecht, M., Schubart, C.D. and Herder, F. (2012) Aquatic biodiversity hotspots in Wallacea: the species flocks in the ancient lakes of Sulawesi, Indonesia. In: Biotic Evolution and Environmental Change in Southeast Asia. (Eds D.J. Gower, K. Johnson, B. Rosen, L. Rüber and S. Williams), pp. 290-315. *Cambridge University Press*, Cambridge.

Vuillemin, A., Friese, A., Alawi, M., Henny, C., Nomosatryo, S., Wagner, D., Crowe, S.A. and Kallmeyer, J. (2016) Geomicrobiological features of ferruginous sediments from Lake Towuti,
Indonesia. *Front Microbiol.*, **7**, 1007. doi: 10.3389/fmicb.2016.01007

Watkinson, I.M. and Hall, R. (2016) Fault systems of the eastern Indonesian triple junction: evaluation of Quaternary activity and implications for seismic hazards. In: Geohazards in

Indonesia: Earth Science for Disaster Risk Reduction (Eds P.R. Cummins and I. Meilano) Geological Society, London, Special Publications, **441**, SP 441-8.

Webb, M., Barker, P.A., Wynn, P.M., Heiri, O., van Hardenbroek, M., Pick, F., Russell, J.M. and Leng, M. (2016) The interpretation of carbon isotope ratios in freshwater diatom silica. *J. Quatern. Sci.*, **31**, 300-309.

Weber, A.K., Russell, J.M., Goudge, T.A., Salvatore, M.R., Mustard, J.F. and Bijaksana, S. (2015) Characterizing clay mineralogy in Lake Towuti, Indonesia, with reflectance spectroscopy. *J. Paleolimnol.*, **54**, 253-261.

Weltje, G.J. (1997) End-member modeling of compositional data: numerical-statistical algorithms for solving the explicit mixing problem. *Math. Geol.*, **29**, 503-549.

Weltje, G.J. and Prins, M.A. (2007) Genetically meaningful decomposition of grain-size distributions. *Sed. Geol.*, **202**, 409-424.

Wennrich, V., Francke, A., Dehnert, A., Juschus, O., Leipe, T., Vogt, C., Brigham-Grette, J., Minyuk, P.S. and Melles, M. (2013) Modern sedimentation patterns in Lake El'gygytgyn, NE Russia, derived from surface sediment and inlet streams samples. *Climate of the Past*, **9**, 135-148.

Wentworth, C.K. (1922) A scale of grade and class terms for clastic sediments. *J. Geology*, **30**, 377-392.

Wilson, M.E. and Moss, S.J. (1999) Cenozoic palaeogeographic evolution of Sulawesi and Borneo. *Palaeogeogr. Palaeoclimatol. Palaeoecol.*, **145**, 303-337.

FIGURE CAPTIONS

Fig.1. (A) Digital elevation model (DEM) of the Lake Towuti area showing the lakes Matano and Mahalona further upstream, the major inlets, the outlet Larona River, the lake bathymetry, and the sampling sites. (B) Location of Lake Towuti (red dot) on Sulawesi Island, south-eastern Asia.

Fig. 2. Geological map, showing the catchment areas of the lakes Towuti, Matano and Mahalona (red lines), along with the names of major settlements (underlined) as well as the inlets and the outlet (blue; after Costa et al., 2015, based on data from PT Vale).

Fig. 3. Scanning electron microscope (SEM) images showing: (A) a single, well-preserved benthic diatom; (B) a sponge spicule with rounded ends and smaller benthic diatoms attached; and (C) a sponge spicule with tip ends.

Fig. 4. Distribution of (A) diatoms; (B) sponge spicules; and (C) tephra particles in the surface sediments of Lake Towuti. The surface sediment samples are indicated by black dots, the International Continental Scientific Drilling Program (ICDP) drill sites by grey circles, and the names of major rivers by abbreviations (*cf*. Fig. 2).

Fig. 5. Distribution of physical properties in the surface sediments of Lake Towuti, with (A) sand; (B) silt; (C) clay contents; (D) the grain-size variations of all 84 samples (grey curves) along with their end-members representing clay (blue) and silt and sand (red); as well as (E) the magnetic susceptibility (MS). In (A) to (C) and (E) the surface sediment samples are

indicated by black dots, the International Continental Scientific Drilling Program (ICDP) drill sites by grey circles and the names of major rivers by abbreviations (*cf*. Fig. 2).

Fig. 6. (A) to (C) Distribution of geochemical properties in the surface sediments of Lake Towuti, reflecting biogenic deposition (TOC, C/N and $\delta^{13}C_{OM}$). (D) to (L) Accumulation of selected major elements (Ti, K, Al, Si, Mg, Ca and Fe) and trace elements (Cr and Mn). For comparison, the elemental composition of river sediments (after Costa et al., 2015) is shown by open circles with the same colour scale as for the surface sediments. The surface sediment samples are indicated by black dots, the International Continental Scientific Drilling Program (ICDP) drill sites by grey circles, and the names of major rivers by abbreviations (*cf*. Fig. 2).

Fig. 7. Distribution of major minerals in the surface sediments of Lake Towuti, comprising the serpentine group with antigorite and greenalite (A) to (C); the clay mineral groups smectite, illite, chlorite and kaolinite (D) to (G); the oxides, quartz and goethite (H) and (I); the amphiboles, tremolite and hornblende (J) and (K); and other minerals (L). The surface sediment samples are indicated by black dots, the International Continental Scientific Drilling Program (ICDP) drill sites by grey circles, and the names of major rivers by abbreviations (*cf*. Fig. 2).

Fig. 8. End-member diagrams of the major and trace elements in the surface sediments of Lake Towuti. (A) Reflecting fluvial supply by the Mahalona River at the northern shore (EM_{Chem} 1). (B) By the Timampu inlets at the northwestern shore and the Loeha River at the eastern shore (EM_{Chem} 2). (C) By the Lengke inlet at the southern shore and the Lemo-Lemo inlet at the north-eastern shore (EM_{Chem} 3). The ICDP drill sites are indicated by grey circles and the names of major rivers by abbreviations (*cf*. Fig. 2).

Fig. 9. Redundancy analysis (RDA) plot showing the surface samples from Lake Towuti, with their water depths indicated by different symbols along with most of the geochemical, physical, and mineralogical data obtained and the geochemical end-members EM_{Chem} 1 to EM_{Chem} 3 (*cf.* Fig. 8).

Supporting Online Material

Fig. S1. Correlation matrix showing the dependency between the geochemical, granulometric, and mineralogical data of the surface samples from Lake Towuti. Note that this table relies on a reduced data set for only those samples, on which all proxies shown were determined; the real correlation coefficients of two proxies can be higher, when all data existing is considered.

Fig. S2. End-member diagrams of the major minerals in the surface sediments of Lake Towuti, reflecting fluvial supply by the Mahalona River at the northern shore – EM_{Min} 1 (A), by the Timampu inlets at the north-western shore and the Loeha River at the eastern shore (EM_{Min} 2 – (B), and by the Lengke inlet at the southern shore and the Lemo–Lemo inlet at the north-eastern shore – EM_{Min} 3 (C). The ICDP drill sites are indicated by grey circles and the names of major rivers by abbreviations (*cf.* Fig. 2).

Table 1. Surface sediment samples from Lake Towuti with their locations and water depths; stars in front of the sample numbers indicate sediment samples that contain organic macro-remains.

Sample number	Longitude	Latitude	Water depth [m]	Sample number	Longitude	Latitude	Water depth [m]
1	121.42	-2.67	6.30	43	121.56	-2.73	141.60
*2	121.44	-2.65	5.40	*44	121.58	-2.73	126.80
3	121.45	-2.67	48.40	45	121.61	-2.73	81.80
4	121.45	-2.69	97.50	46	121.61	-2.74	53.80
*5	121.48	-2.65	47.10	47	121.60	-2.75	73.90
6	121.48	-2.67	7.50	48	121.60	-2.76	92.20
7	121.45	-2.67	62.40	*49	121.59	-2.76	25.60
8	121.52	-2.67	49.00	50	121.59	-2.78	4.50
9	121.53	-2.68	96.40	*51	121.57	-2.80	4.40
10	121.52	-2.67	72.60	*52	121.57	-2.78	32.90
11	121.51	-2.68	83.40	53	121.57	-2.76	73.20
12	121.52	-2.69	124.70	54	121.56	-2.74	129.60
13	121.55	-2.68	140.00	*55	121.54	-2.76	96.00
*14	121.53	-2.69	125.40	*56	121.51	-2.75	134.90
*15	121.56	-2.67	171.20	57	121.59	-2.78	58.90
*16	121.56	-2.69	174.90	58	121.48	-2.76	127.60
*17	121.59	-2.70	195.50	59	121.48	-2.79	112.00
18	121.53	-2.67	3.50	*60	121.47	-2.82	134.30
19	121.49	-2.69	123.70	*61	121.44	-2.83	117.60
20	121.44	-2.70	75.60	*62	121.44	-2.86	117.50
21	121.48	-2.70	144.70	63	121.42	-2.87	119.60
*22	121.56	-2.70	171.40	*64	121.40	-2.89	77.50
23	121.59	-2.68	177.90	*65	121.39	-2.93	19.10
24	121.64	-2.68	133.30	66	121.41	-2.92	40.70
25	121.66	-2.70	129.20	67	121.43	-2.91	120.80
26	121.63	-2.72	137.70	68	121.45	-2.88	168.80
27	121.66	-2.73	59.30	69	121.48	-2.86	177.00
28	121.61	-2.71	194.50	70	121.48	-2.84	152.00
29	121.58	-2.71	172.10	71	121.50	-2.81	132.00
30	121.54	-2.71	147.60	72	121.51	-2.78	71.60
31	121.52	-2.71	147.40	73	121.46	-2.91	87.10
32	121.49	-2.72	153.70	*74	121.48	-2.90	93.30
33	121.47	-2.72	100.40	75	121.50	-2.88	50.60
34	121.56	-2.72	141.10	76	121.50	-2.86	160.00
35	121.54	-2.72	154.00	77	121.53	-2.85	53.40
36	121.51	-2.73	157.70	78	121.51	-2.83	119.00
37	121.48	-2.73	146.50	79	121.55	-2.83	46.80
38	121.46	-2.74	78.50	80	121.53	-2.81	99.80
*39	121.66	-2.66	101.10	81	121.46	-2.84	168.50
40	121.46	-2.75	101.20	*82	121.44	-2.93	36.10
*41	121.50	-2.74	130.10	83	121.40	-2.93	2.80
*42	121.52	-2.74	161.80	*84	121.54	-2.87	9.60

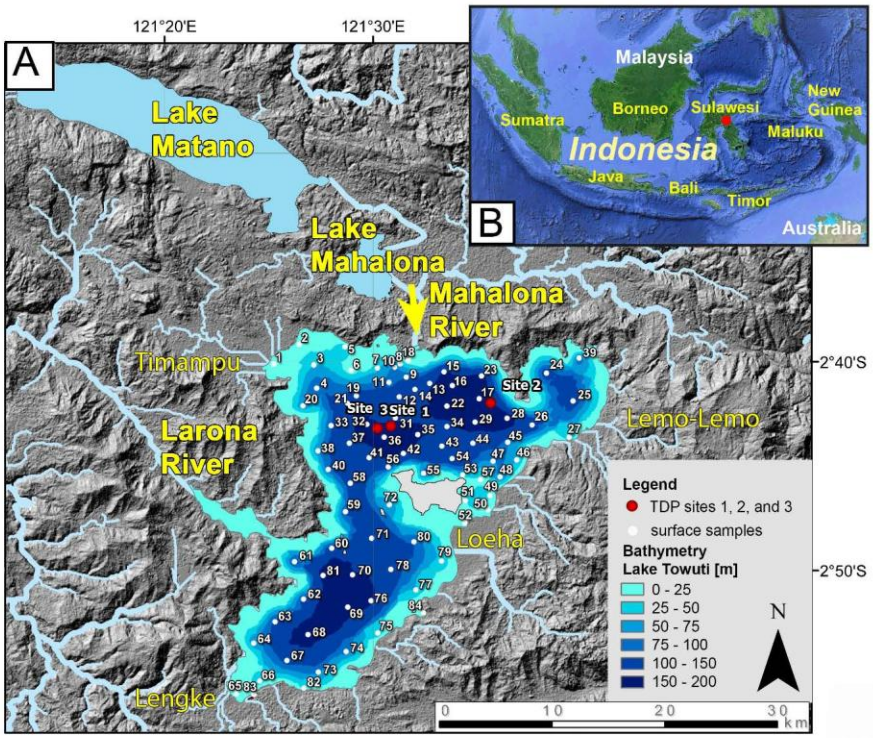

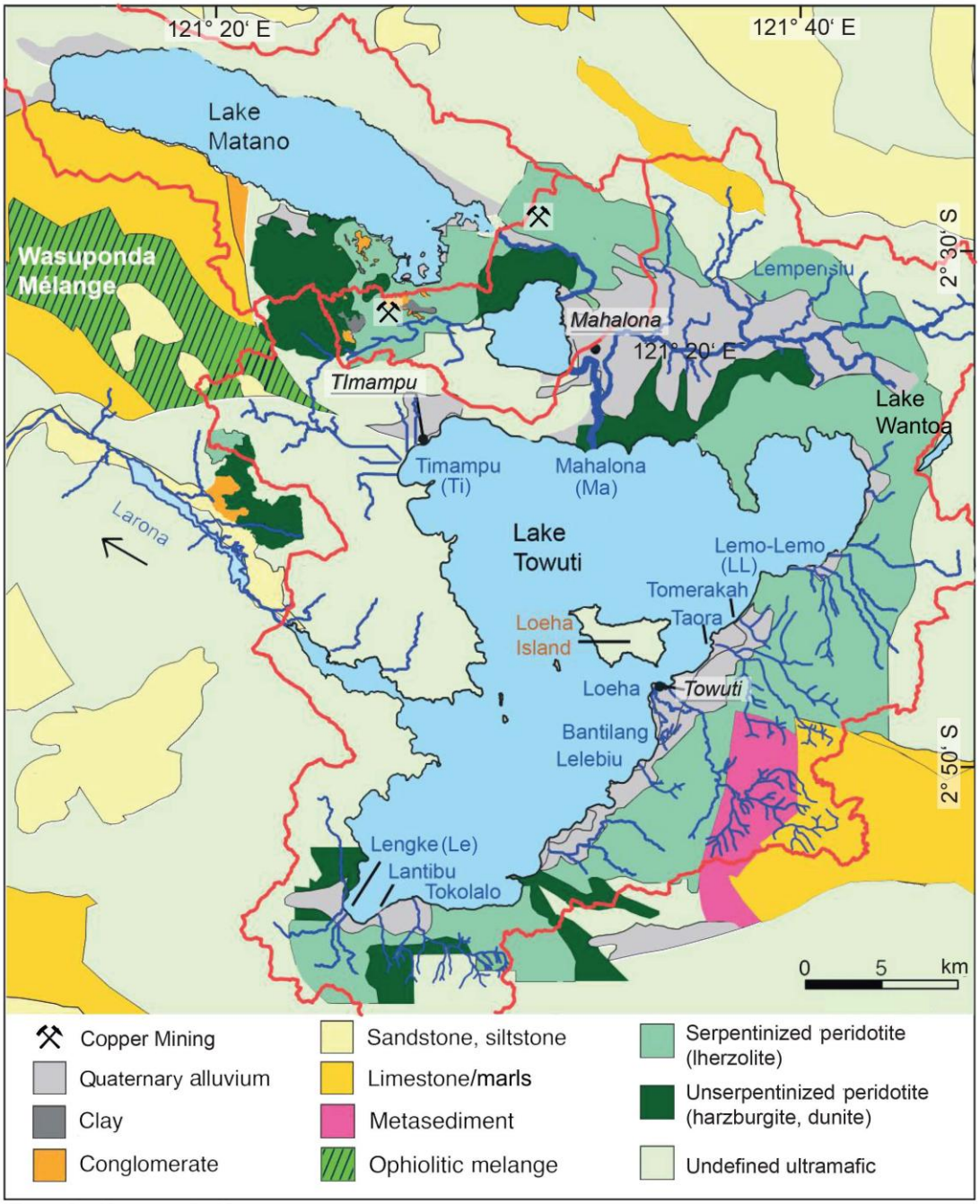

Figure 2: [Hasberg et al.]

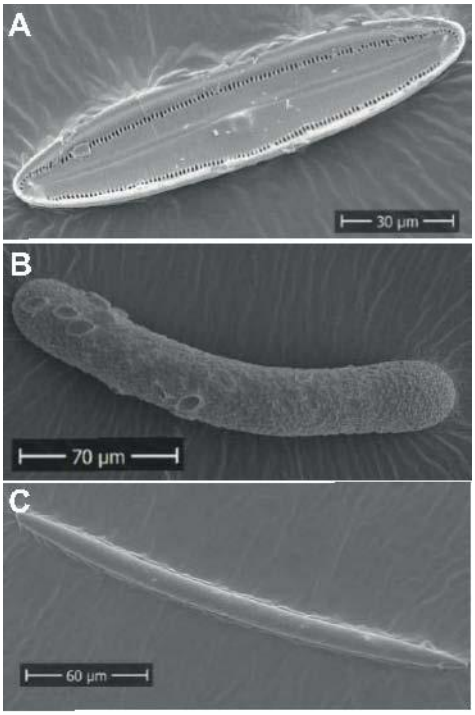

Figure 3: (A), (B), and (C) [Hasberg et al.]

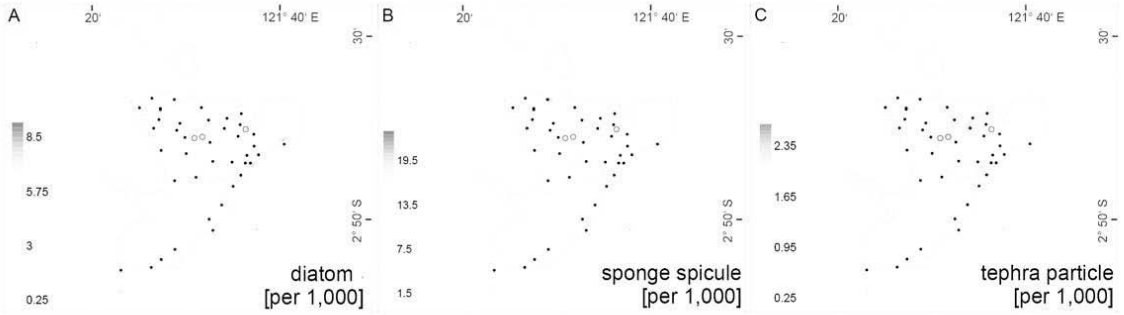

Figure 4: (A), (B), and (C) [Hasberg et al.]

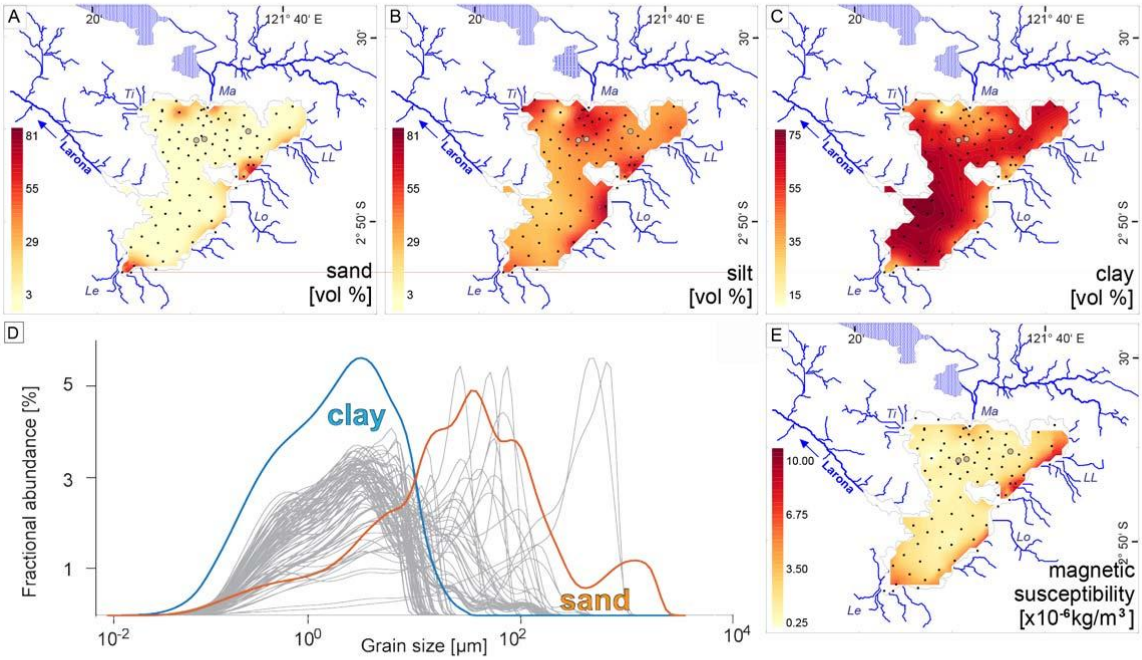

Figure 5: (A), (B), (C), (D), and (E)
[Hasberg et al.]

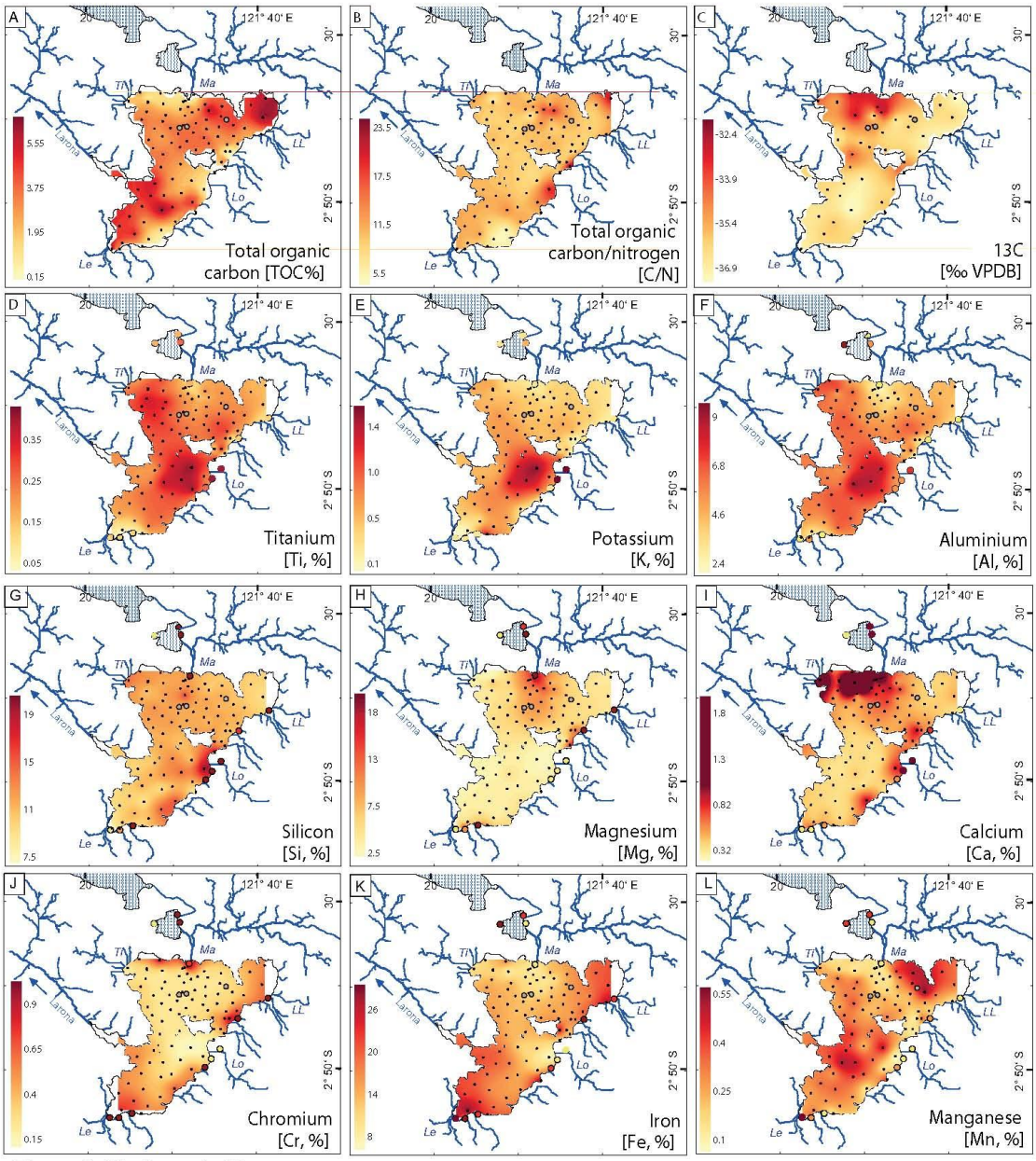

Figure 6: [Hasberg et al.]

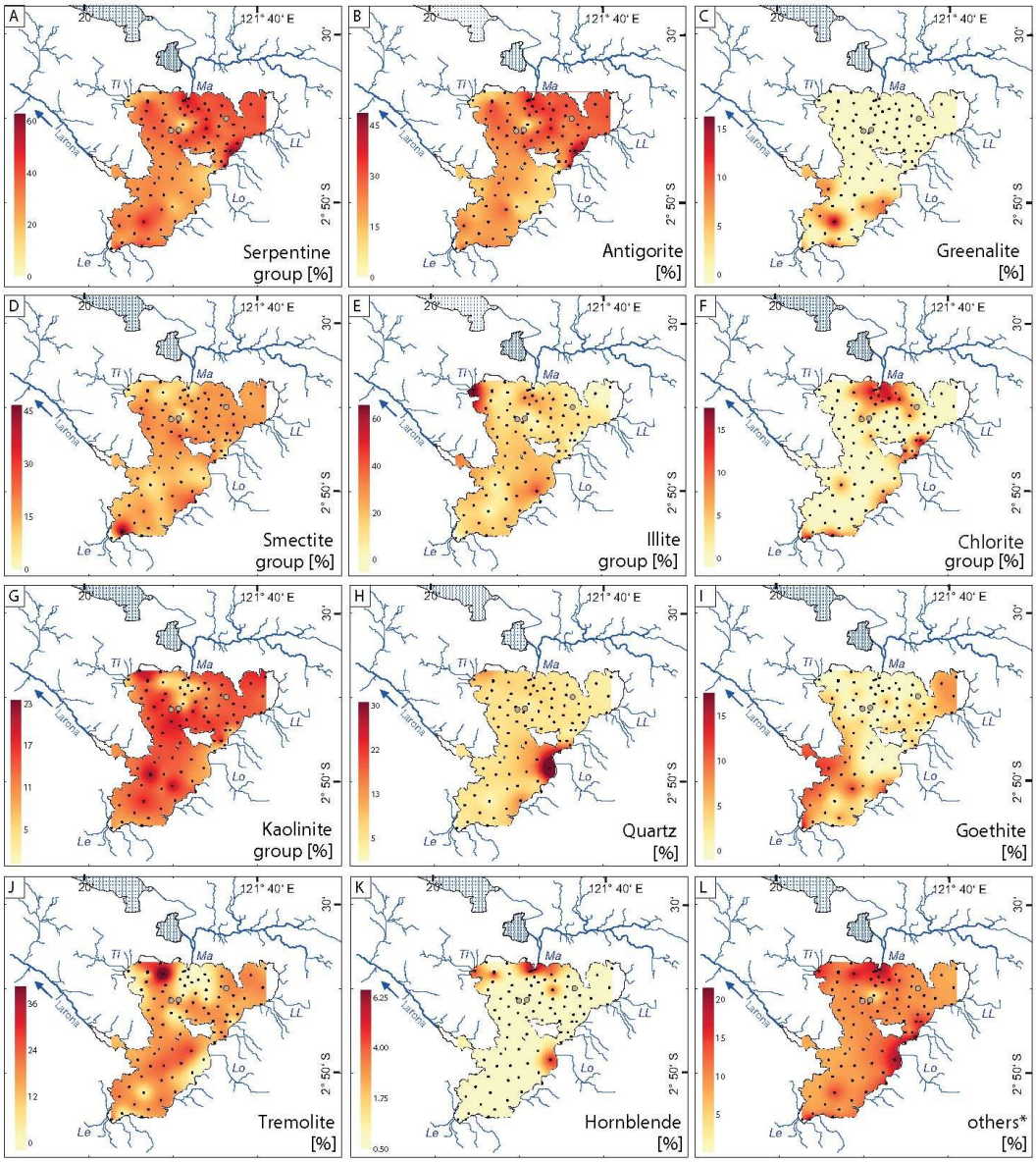

Figure 7:
[Hasberg et al.]

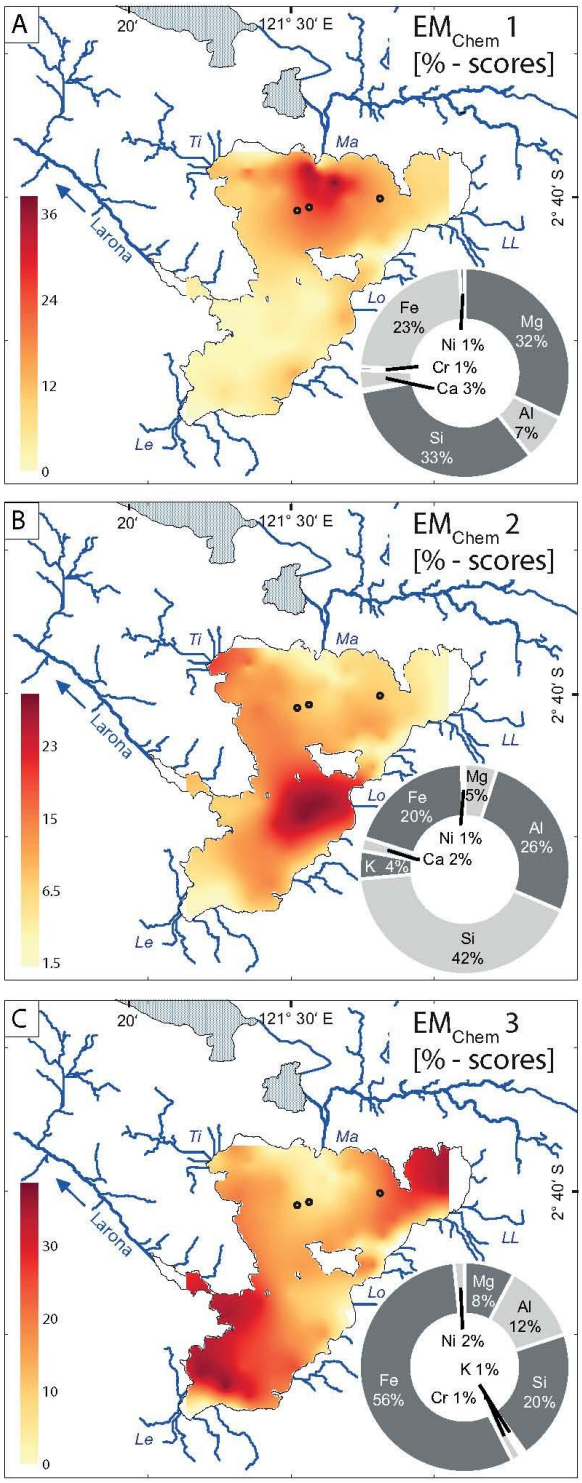

Figure 8: (A), (B), and (C) [Hasberg et al.]

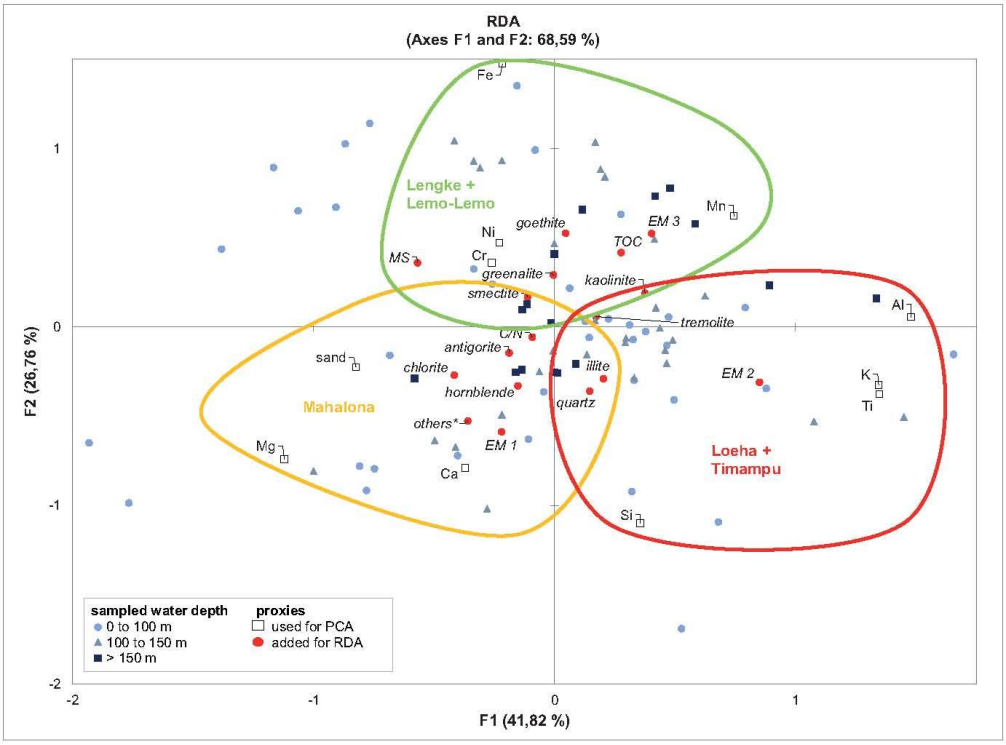

Figure 9:
[Hasberg et al.]